Notes on

High Voltage Technique

by

Sivaji Chakravorti

Numerical Computation of Electric Field

Introduction

The design of the insulation of high voltage apparatus between phases and earth and also between the phases is based on the knowledge of electric field distribution and the dielectric properties of the combination of insulating materials used in the system. The principal aim is that the insulation should withstand the electric stresses with adequate reliability and at the same time the insulation should not be over dimensioned.
It is well known that the withstand voltage of the external insulation of apparatus designed with non-self restoring insulation is determined by the maximum value of electric field intensity within the insulation system. Further, corona discharges are eliminated by proper design of high voltage shielding electrodes. Thus a comprehensive study of the electric field distribution in and around high voltage equipment is of great practical importance.
High voltage equipments, in practice, are in most of the cases subjected to a.c. field of frequency 50Hz or 60Hz. These fields may be approximated as quasi-static as the wavelength is much longer compared to the dimension of the components involved. Because of this, the electrostatic field calculation is possible by the different methods in use.

Mathematically, an electric field calculation problem may be formulated as follows:

The purpose is to determine, at each point within the field region of interest, the value of potential $\phi(x,y,z)$ and that of the electric field intensity $\vec{E}(x, y, z)$ are to be determined, which are related as

$$\vec{E}(x, y, z) = -\vec{\nabla}\phi \qquad \text{…. 13.1}$$

In order to do that either the Laplace's Equation for systems without any source of charge in the field region,

$$\vec{\nabla}^2\phi = 0 \qquad \text{…. 13.2}$$

or, the Poisson's Equation for systems with sources of charge in the field region,

$$\vec{\nabla}^2\phi = -\frac{\rho_v}{\varepsilon} \qquad \text{…. 13.3}$$

are required to be solved.

The solutions of these equations are called Boundary Value problems, whereby the boundary conditions are specified by means of the given potential of electrode (Dirichlet's Problem) or by the given value of electric field intensity (Neumann's Problem).

Methods of Determination of Electric Field Distribution

The methods that are employed for determination of electric field are detailed in Fig.13.1.

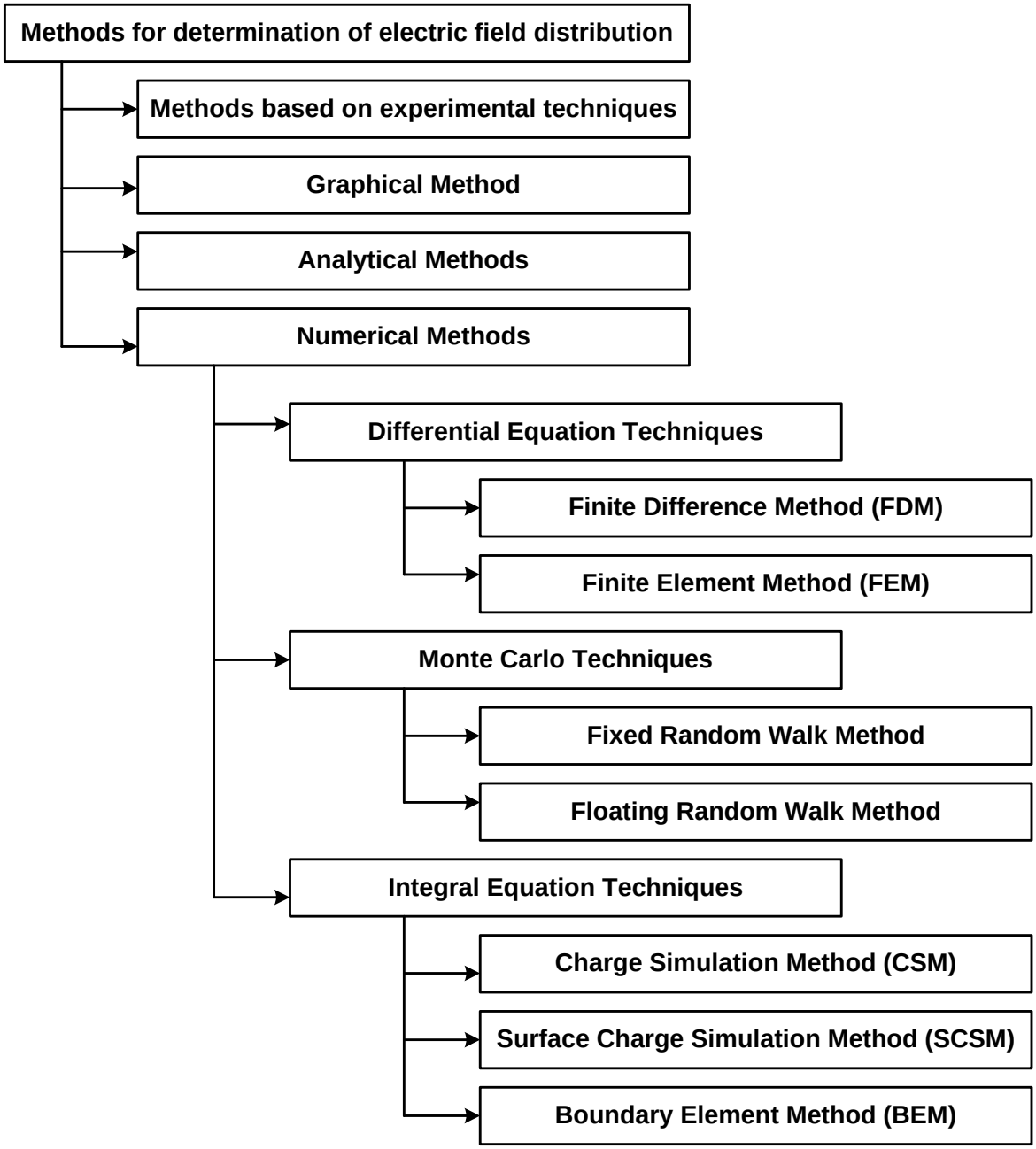

Fig. 13.1 Different methods for determination of electric field distribution

The analytical methods can only be applied to the cases, where the electrode or dielectric boundaries are of simple geometrical forms such as cylinders, spheres etc. In other words, in this method the boundaries are required to be defined exclusively by known mathematical functions. The results obtained are very accurate. But, as it is obvious, this method cannot be applied to complex problems. However, the results obtained by analytical methods for standard configurations are used still today to validate the results obtained by some other approximate methods such as numerical methods.

Earlier the experimental as well as the graphical methods were used to get a fair idea about the nature of field distribution in some practical cases. However, these methods are greatly

limited in their areas of usage and the errors involved are usually very high for any complex problem to be taken directly for design purposes.
In more and more engineering problems now-a-days, it is found that it is necessary to obtain approximate numerical solutions rather than exact closed-form solutions. The governing equations and boundary conditions for these problems could be written without too much effort, but it may be seen immediately that no simple analytical solution can be found. The difficulty in these engineering problems lies in the fact that either the geometry or some other feature of the problem is irregular. Analytical solutions to this type of problems seldom exist; yet these are the kinds of problems that engineers need to solve.
There are several alternatives to overcome this dilemma. One possibility is to make simplifying assumptions ignoring the difficulties to reduce the problem to one that can be easily handled. Sometimes this approach works; but, more often than not, it leads to serious inaccuracies. With the availability of computers today, a more viable alternative is to retain the complexities of the problem and find an approximate numerical solution.
Several approximate numerical analysis methods have evolved over the years as shown in Fig.13.1. For each practical field problem, depending upon the dielectric properties, complexity of contours and boundary conditions, one or the other numerical method is more suited.

Uniqueness Theorem

It states that once any method of solving Poisson's or Laplace's equations subject to given boundary conditions has been found, the problem has been solved once and for all. No other method can ever give a different solution.

Proof:
Consider a volume V bounded by a surface S. Also consider that there is a charge density ρ_v throughout the volume V, and the value of the scalar electric potential on the surface S is ϕ_s. Assume that there are two solutions of Poisson's equation, viz. ϕ_1 and ϕ_2. Then

$$\vec{\nabla}^2\phi_1 = -\frac{\rho_v}{\varepsilon} \quad \text{and} \quad \vec{\nabla}^2\phi_2 = -\frac{\rho_v}{\varepsilon}$$

So, $\vec{\nabla}^2(\phi_1 - \phi_2) = 0$ …. 13.4

Now, each solution must also satisfy the boundary conditions. It is to be noted here that one particular point can not have two different electric potentials, as the work done to move a unit positive charge from infinity to that point is unique. Let, the value of ϕ_1 on the boundary is ϕ_{1s} and the value of ϕ_2 on the boundary is ϕ_{2s} and they must be identical to ϕ_s.
Therefore, $\phi_{1s} = \phi_{2s} = \phi_s$
or, $\phi_{1s} - \phi_{2s} = 0$
For any scalar ϕ and any vector $\vec{D}$, the following vector identity can be written.

$$\vec{\nabla}(\phi\vec{D}) \equiv \phi(\vec{\nabla}.\vec{D}) + \vec{\nabla}\phi.\vec{D} \quad \text{…. 13.5}$$

Consider the scalar as $(\phi_1 - \phi_2)$ and the vector as $\vec{\nabla}(\phi_1 - \phi_2)$. Then from identity (13.5),

$$\vec{\nabla}.\left[(\phi_1 - \phi_2)\vec{\nabla}(\phi_1 - \phi_2)\right] \equiv (\phi_1 - \phi_2)\left[\vec{\nabla}.\vec{\nabla}(\phi_1 - \phi_2)\right] + \vec{\nabla}(\phi_1 - \phi_2).\vec{\nabla}(\phi_1 - \phi_2) \quad \text{…. 13.6}$$

Now, integrating throughout the volume V enclosed by the boundary surface S,

$$\int_V \vec{\nabla}.\left[(\phi_1-\phi_2)\vec{\nabla}(\phi_1-\phi_2)\right]dv \equiv \int_V (\phi_1-\phi_2)\left[\vec{\nabla}.\vec{\nabla}(\phi_1-\phi_2)\right]dv + \int_V \vec{\nabla}(\phi_1-\phi_2).\vec{\nabla}(\phi_1-\phi_2)dv$$
$$\equiv \int_V (\phi_1-\phi_2)\left[\vec{\nabla}^2(\phi_1-\phi_2)\right]dv + \int_V \left[\vec{\nabla}(\phi_1-\phi_2)\right]^2 dv \quad \text{…. 13.7}$$

Applying divergence theorem to the L.H.S of identity (13.7),

$$\int_V \vec{\nabla}.\left[(\phi_1-\phi_2)\vec{\nabla}(\phi_1-\phi_2)\right]dv = \int_S (\phi_{1S}-\phi_{2S})\vec{\nabla}(\phi_1-\phi_2)ds = 0 \quad \text{…. 13.8}$$

as $\phi_{1s} = \phi_{2s}$ on the specified surface *S*.

On the RHS of identity (13.7), $\vec{\nabla}^2(\phi_1-\phi_2) = 0$ from eqn.(13.4). Hence, identity (13.7) reduces to

$$\int_V \left[\vec{\nabla}(\phi_1-\phi_2)\right]^2 dv = 0 \quad \text{…. 13.9}$$

Since, $\left[\vec{\nabla}(\phi_1-\phi_2)\right]^2$ cannot be negative, hence the integrand must be zero everywhere so that the integral may be zero.

Hence,

$$\left[\vec{\nabla}(\phi_1-\phi_2)\right]^2 = 0 \qquad \text{or, } \vec{\nabla}(\phi_1-\phi_2) = 0 \quad \text{…. 13.10}$$

Again, if the gradient of $(\phi_1 - \phi_2)$ is zero everywhere, then

$$\phi_1 - \phi_2 = Constant \quad \text{…. 13.11}$$

This constant may be evaluated by considering a point on the boundary surface *S*. So that,

$$\phi_1 - \phi_2 = \phi_{1s} - \phi_{2s} = 0$$

or, $\phi_1 = \phi_2$

which means that the two solutions are identical.

However, in practice if the same problem is solved by using different numerical techniques the results are not exactly the same. This is due to the fact that the errors in a particular numerical method are often problem dependent and hence the results are not exactly same in all the methods. So, this is not a violation of the Uniqueness theorem.

Procedural Steps in Numerical Electric Field Computation

The following are the procedural steps that need to be followed not only for FDM but for most of the numerical electric field computation methods.

At first, the Region of Interest (ROI) needs to be identified. ROI is the region where the solution for electric field is to be obtained. For example, normally the field solution is not needed within the electrode volume or below the earth surface. Hence, for an isolated electrode and the earth surface, the ROI will be region between the electrode surface and the earth surface as shown in Fig.13.2. Before the ROI is identified, the geometries of the components that comprise the field system need to be defined. This step is now-a-days done with the help of CAD software.

The subsequent procedural step is to discretize the entire ROI or the boundaries to create the nodes where the solution of field will be obtained. Ideally one should find the field solution at each and every point within the ROI. But it will result in immense computational burden and hence the field solution is obtained at discrete nodes. This step is called Discretization and is often done with the help of mesh generators, which are software modules that create the mesh within the entire ROI or on the boundaries. In order that the electric field solution can be obtained at any specific location within the ROI, a pre-defined variation of electric field between successive nodes is assumed. In fact, this assumption is a root cause of inaccuracy of the numerical method.

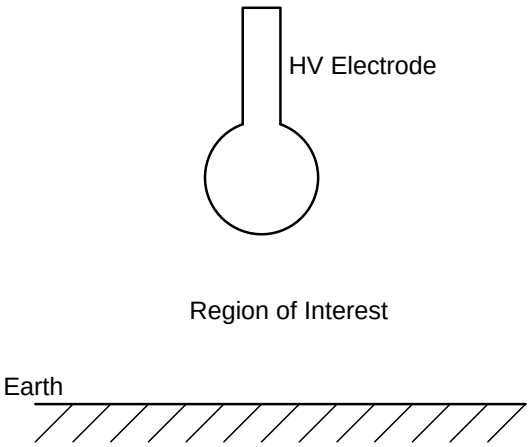

Fig. 13.2 Depiction of Region of Interest for Electric Field Computation

The next step is to create the system of equations based on the numerical method that is being employed. Subsequently, the system of equations is solved using a suitable solver. The solver needs to be chosen depending upon the nature of the coefficient matrix that is being created by the specific numerical method. This solution gives the results for the unknown field quantities at the pre-defined nodes. Finally the results at any desired location is computed using the assumed variation of electric field between the nodes, which is termed as post processing of results. The procedural steps are depicted in Fig.13.3.

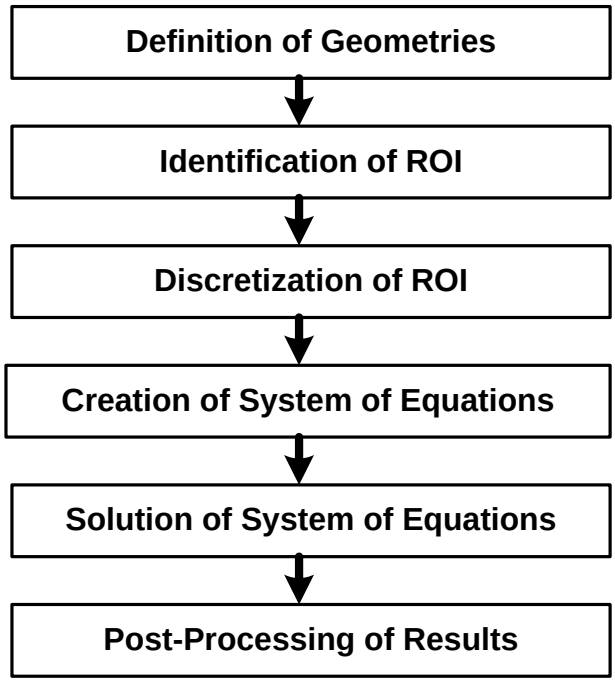

Fig. 13.3 Procedural steps in numerical electric field computation

FINITE DIFFERENCE METHOD

A) Two Dimensional System with equal nodal distance:

In a 2-D system, V is independent of one of the axis directions, e.g. in the case of cable V is taken to be independent of z-direction, where z is along the length of the cable. Then the Laplace's equation is written as -

$$\frac{\partial^2 V}{\partial x^2} + \frac{\partial^2 V}{\partial y^2} = 0 \qquad (1)$$

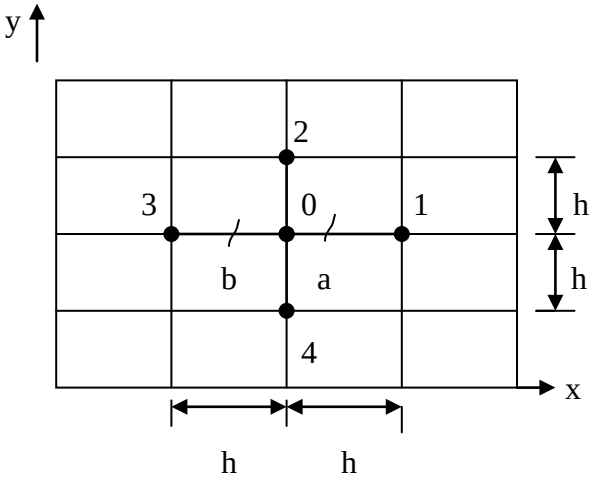

In FDM V_o is expressed in terms of the potentials of the connected nodes, i.e. V_1, V_2, V_3 and V_4, such that Laplace's equation is satisfied at the point "0".

Let, a and b be the mid-points between 0 & 1 and 3 & 0 respectively. Then according to mean value theorem

$$\left(\frac{\partial V}{\partial x}\right)_a = \frac{V_1 - V_o}{h} \qquad (2)$$

and $$\left(\frac{\partial V}{\partial x}\right)_b = \frac{V_o - V_3}{h} \qquad (3)$$

Again, 0 being the mid-point between a and b,

$$\left(\frac{\partial^2 V}{\partial x^2}\right)_o = \frac{\left(\frac{\partial V}{\partial x}\right)_a - \left(\frac{\partial V}{\partial x}\right)_b}{h}$$

$$= \frac{V_1 + V_3 - 2V_o}{h^2} \quad (4)$$

similarly, $\left(\frac{\partial^2 V}{\partial y^2}\right)_o = \frac{V_2 + V_4 - 2V_o}{h^2}$ (5)

Now, satisfying Laplace's equation at "0"

$$\left(\frac{\partial^2 V}{\partial x^2}\right)_o + \left(\frac{\partial^2 V}{\partial y^2}\right)_o = 0$$

or, $\frac{V_1 + V_3 - 2V_o}{h^2} + \frac{V_2 + V_4 - 2V_o}{h^2} = 0$

or $V_o = \frac{1}{4}(V_1 + V_2 + V_3 + V_4)$ (6)

Proof applying Taylor's Series:

Taylor's Series

$$f(x+a, y+b) = f(x,y) + a\frac{\partial}{\partial x} f(x,y) + b\frac{\partial}{\partial y} f(x,y) + \frac{a^2}{2!}\frac{\partial^2}{\partial x^2} f(x,y) + \frac{b^2}{2!}\frac{\partial^2}{\partial y^2} f(x,y) + ... \quad (7)$$

Applying this series between the nodes 0 and 1, i.e. a=h and b=0,

$$V_1 = V_o + h\left(\frac{\partial V}{\partial x}\right)_o + \frac{h^2}{2!}\left(\frac{\partial^2 V}{\partial x^2}\right)_o + ... \quad (8)$$

Similarly, between the nodes 3 and 0, i.e. a = - h and b = 0. So,

$$V_3 = V_o - h\left(\frac{\partial V}{\partial x}\right)_o + \frac{h^2}{2!}\left(\frac{\partial^2 V}{\partial x^2}\right)_o - \ldots\ldots \qquad (9)$$

Neglecting higher powers of h, as h is small and adding (8) and (9),

$$V_1 + V_3 = 2V_o + h^2\left(\frac{\partial^2 V}{\partial x^2}\right)_o$$

or, $$\left(\frac{\partial^2 V}{\partial x^2}\right)_o = \frac{V_1 + V_3 - 2V_o}{h^2} \qquad (10)$$

Similarly, applying Taylor's series between the nodes 2, 0 and 4, it can be proved that

$$\left(\frac{\partial^2 V}{\partial y^2}\right)_o = \frac{V_2 + V_4 - 2V_o}{h^2} \qquad (11)$$

Then, satisfying Laplace's equation at "0", it may be obtained that

$$V_o = \frac{1}{4}\left(V_1 + V_2 + V_3 + V_4\right) \qquad (12)$$

Simple Example

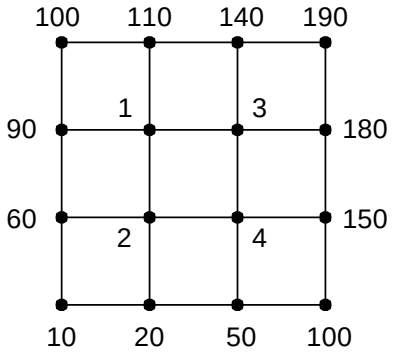

FDM equations

$V_1 = ¼ (V_2 + V_3 + 90 + 110)$

$V_2 = ¼ (V_1 + V_4 + 60 + 20)$

$V_3 = ¼ (V_1 + V_4 + 140 + 180)$ and

$V_4 = ¼ (V_2 + V_3 + 50 + 150)$

Acceleration of Convergence by over-relaxation:

It has been found that successive over-relaxation proposed independently by Frankel and Young can have very rapid convergence, e.g. a problem that may require 840 iterations by simple Gauss- Seidal method will take only about 70 iteration by this acceleration technique. This technique proposes that

$$V = V_{calc} + (a - 1) (V_{calc} - V_{old}) \quad (13)$$

V_{calc} is the calculated value from Laplace's equation

V_{old} is the value from previous iteration

a is the acceleration factor

V is the value of the node potential.

The value of a is always $2 > a > 1$.

Equation (13) can be rewritten as

$$V = V_{old} + a (V_{calc} - V_{old}) \quad (14)$$

Equation (14) thus implies that if there is a tendency of a node potential to increase from the value of the earlier iteration, then node potential to be taken in this iteration is above the calculated value by a certain fraction of the increment, as $2 > a > 1$.

At the final iteration, where the convergence criterion is met, the difference from the previous iteration will be very small and, hence, there will be negligible deviation from the calculated value. However, the number of iterations required to achieve convergence depends heavily on the choice of acceleration factor.

For Laplace's equation empirical results show that optimum value of acceleration factor "a" for a square field region with (p+1) nodes along each side is given by

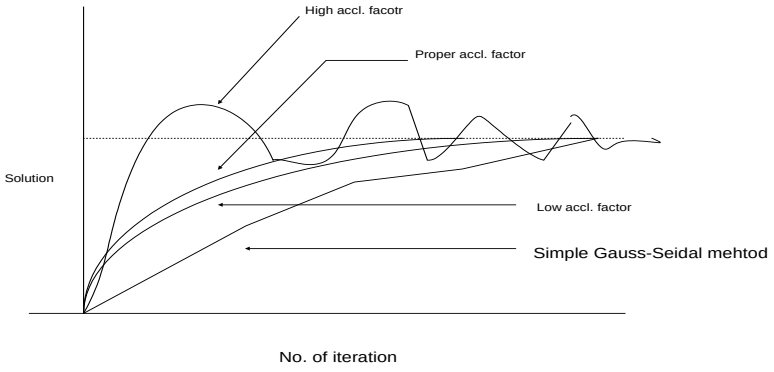

$$a = \frac{2}{1+\sin\frac{\pi}{p}} \tag{15}$$

For rectangular region with (p+1) x (q+1) nodes

$$a = 2\left\{1-\pi\sqrt{\frac{1}{2}\left(\frac{1}{p^2}+\frac{1}{q^2}\right)}\right\} \tag{16}$$

where , p and q are greater than 15.

For p = q > 15,

$$a = 2\left(1-\frac{\pi}{p}\right) \tag{17}$$

Equation (17) also follows from equation (15), because π/p being small,

$\sin\frac{\pi}{p} \approx \frac{\pi}{p}$. Thus, from equation (15)

$$a = \frac{2}{1+\pi/p} = 2\left(1+\pi/p\right)^{-1} \cong 2\left(1-\frac{\pi}{p}\right) \text{ as } \frac{\pi}{p} \langle\langle 1$$

Problem

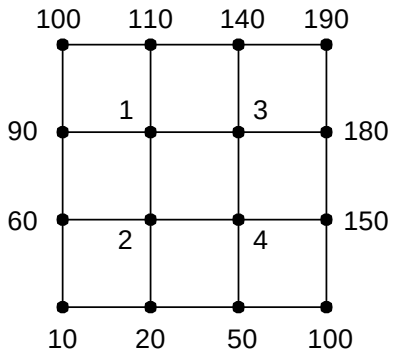

$V_1^{calc} = ¼ (V_2 + V_3)+50$

$V_2^{calc} = ¼ (V_1 + V_4)+20$

$V_3^{calc} = ¼ (V_1 + V_4)+80$

$V_4^{calc} = ¼ (V_2 + V_3)+50$

Here, p+1 = 4 or, p = 3

$$\therefore \text{ Accl.factor}\,(a) = \frac{2}{1+\sin \pi/3} = 1.072$$

For iteration 1:

$$V_1 = V_1^{calc} + (a-1)\left(V_1^{calc} - V_1^{old}\right)$$

$$= 50 + (1.072-1)(50-0) = 53.6$$

$$V_2 = V_2^{calc} + (a-1)\left(V_2^{calc} - V_2^{old}\right)$$

Now, $V_2^{calc} = \frac{1}{4}(53.6+0)+20 = 33.4$

$$\therefore V_2 = 33.4 + (1.072-1)(33.4-0) = 35.8$$

and so on.

B) Two-dimensional system with unequal nodal distance:

Near electrode or dielectric boundaries, the nodal distances may not be equal. As shown in the diagram

$S_1, S_2, S_3, S_4 < 1.$

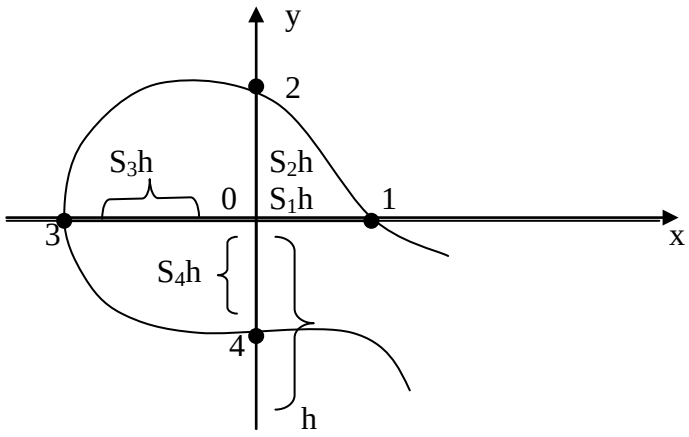

In the Taylor series expansion between the nodes 0 and 1, a = S_1h and b = 0. So,

$$V_1 = V_o + S_1 h\left(\frac{\partial V}{\partial x}\right)_o + \frac{S_1^2 h^2}{2}\left(\frac{\partial^2 V}{\partial x^2}\right)_o +,..... \qquad (18)$$

and between the nodes 3 and 0, a = - S_3h and b = 0.

$$V_3 = V_o - S_3 h\left(\frac{\partial V}{\partial x}\right)_o + \frac{S_3^2 h^2}{2}\left(\frac{\partial^2 V}{\partial x^2}\right)_o -,..... \qquad (19)$$

Hence,

$$\frac{V_1}{S_1} + \frac{V_3}{S_3} = V_o\left(\frac{1}{S_1} + \frac{1}{S_3}\right) + \left(\frac{S_1 h^2 + S_3 h^2}{2}\right)\left(\frac{\partial^2 V}{\partial x^2}\right)_o$$

or,
$$\left(\frac{\partial^2 V}{\partial x^2}\right)_o = \frac{\frac{V_1}{S_1} + \frac{V_3}{S_3} - V_o\left(\frac{1}{S_1} + \frac{1}{S_3}\right)}{\frac{h^2}{2}(S_1 + S_3)} \qquad (20)$$

Similarly,

$$\left(\frac{\partial^2 V}{\partial y^2}\right)_o = \frac{\frac{V_2}{S_2} + \frac{V_4}{S_4} - V_o\left(\frac{1}{S_2} + \frac{1}{S_4}\right)}{\frac{h^2}{2}(S_2 + S_4)} \qquad (21)$$

As per Laplace's equation at "0"

$$\left(\frac{\partial^2 V}{\partial x^2}\right)_o + \left(\frac{\partial^2 V}{\partial y^2}\right)_o = 0$$

$$\text{or,} \quad \frac{1}{S_1 + S_3}\left(\frac{V_1}{S_1} + \frac{V_3}{S_3}\right) + \frac{1}{S_2 + S_4}\left(\frac{V_2}{S_2} + \frac{V_4}{S_4}\right) = V_o\left(\frac{1}{S_1 S_3} + \frac{1}{S_2 S_4}\right)$$

$$\text{or,} \quad V_o = \frac{\frac{1}{S_1 + S_3}\left(\frac{V_1}{S_1} + \frac{V_3}{S_3}\right) + \frac{1}{S_2 + S_4}\left(\frac{V_2}{S_2} + \frac{V_4}{S_4}\right)}{\frac{1}{S_1 S_3} + \frac{1}{S_2 S_4}} \qquad (22)$$

Problem

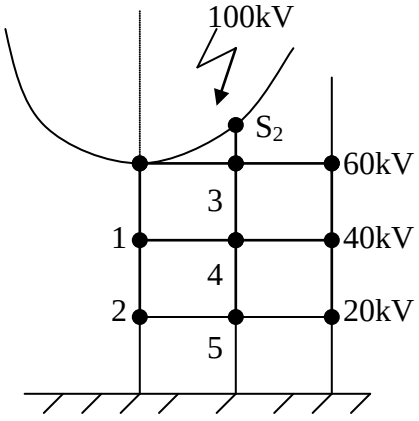

$S_2 = 0.5$, other constants are 1. Because of symmetry, it may be written that $V_1 = ¼ (100 + V_4 + V_2 + V_4)$

or,

$$V_1 = \frac{1}{4}\left(2V_4 + V_2\right) + 25$$

$$V_2 = \frac{1}{4}\left(2V_5 + V_1\right)$$

For V_3, $\quad S_1 = S_3 = S_4 = 1, \quad$ but $S_2 = 0.5$

$$\therefore V_3 = \frac{\frac{1}{2}\left(60 + 100\right) + \frac{1}{1+0.5}\left(\frac{100}{0.5} + \frac{V_4}{1}\right)}{1 + \frac{1}{0.5}}$$

or, $V_3 = 0.22V_4 + 71.1$

Again,

$$V_4 = \frac{1}{4}\left(V_1 + V_3 + V_5\right) + 10$$

and $\quad V_5 = \frac{1}{4}\left(V_2 + V_4\right) + 5$

C) 3-D System with equal nodal distance:

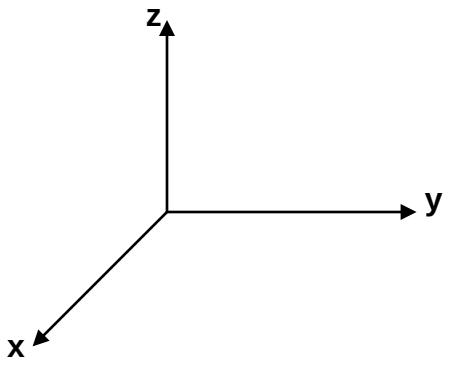

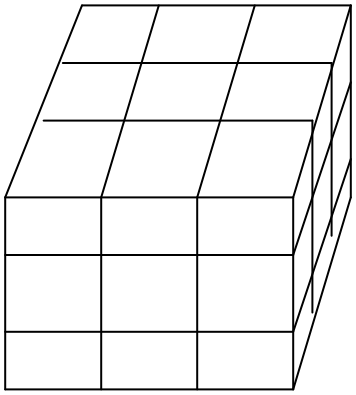

The 3-D field region has to be divided into a large number of cubic elements

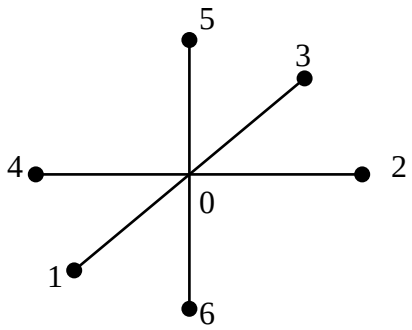

$$\left(\frac{\partial^2 V}{\partial x^2}\right)_o = \frac{V_1 + V_3 - 2V_o}{h^2}$$

$$\left(\frac{\partial^2 V}{\partial y^2}\right)_o = \frac{V_2 + V_4 - 2V_o}{h^2}$$

$$\left(\frac{\partial^2 V}{\partial z^2}\right)_o = \frac{V_5 + V_6 - 2V_o}{h^2}$$

Thus, satisfying Laplace's Eqn. at "0",

$$V_o = \frac{1}{6}\left(V_1 + V_2 + V_3 + V_4 + V_5 + V_6\right) \qquad (6)$$

or, $V_o = \frac{1}{6}\sum_{n=1}^{6} V_n$

D) Axi-symmetric System with Equal Nodal Distance

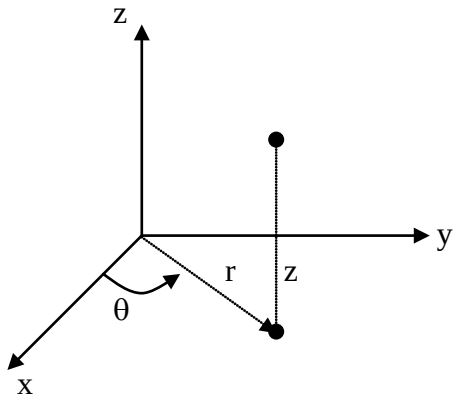

For axi-symmetric system, if the values of r and z are kept constant, then the potential remains same for any value of θ. Thus the potential is a function of r and z only, where z is the axis of symmetry.

Laplace's equation is cylindrical co-ordinates (r,θ,z):

$$\frac{\partial^2 V}{\partial r^2}+\frac{1}{r}\frac{\partial V}{\partial r}+\frac{1}{r^2}\frac{\partial^2 V}{\partial \theta^2}+\frac{\partial^2 V}{\partial z^2}=0 \qquad (24)$$

In axi-symmetric system, V is independent of θ, so that Eqn.(24) reduces to

$$\frac{\partial^2 V}{\partial r^2}+\frac{1}{r}\frac{\partial V}{\partial r}+\frac{\partial^2 V}{\partial z^2}=0 \qquad (25)$$

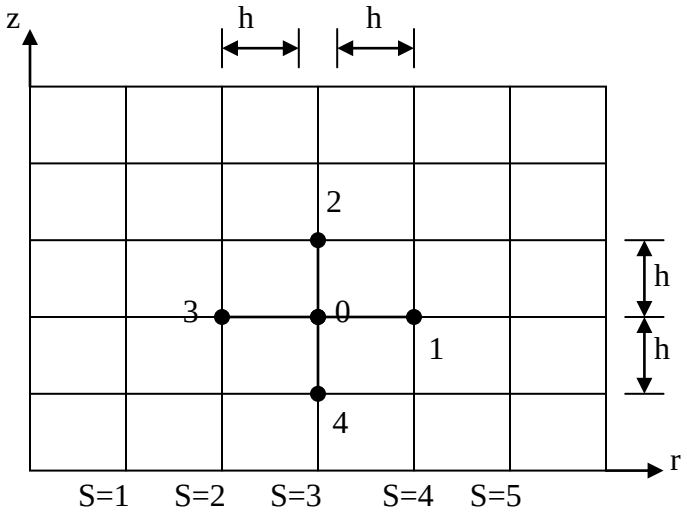

From Taylor's series between 0 and 1,

$$V_1 = V_o + h\left(\frac{\partial V}{\partial r}\right)_o + \frac{h^2}{2}\left(\frac{\partial^2 V}{\partial r^2}\right)_o \qquad (26)$$

and between 3 and 0

$$V_3 = V_o - h\left(\frac{\partial V}{\partial r}\right)_o + \frac{h^2}{2}\left(\frac{\partial^2 V}{\partial r^2}\right)_o \qquad (27)$$

so,

$$V_1 + V_3 = 2V_o + h^2\left(\frac{\partial^2 V}{\partial r^2}\right)_o$$

$$\text{or,} \quad \left(\frac{\partial^2 V}{\partial r^2}\right)_o = \frac{V_1 + V_3 - 2V_o}{h^2} \tag{28}$$

Again, subtracting (27) from (26),

$$V_1 - V_3 = 2h\left(\frac{\partial V}{\partial r}\right)_o$$

$$\text{or,} \quad \left(\frac{1}{r}\frac{\partial V}{\partial r}\right)_o = \frac{1}{Sh}\cdot\frac{V_1 - V_3}{2h}, \quad \text{as } r = Sh$$

$$= \frac{V_1 - V_3}{2Sh^2} \tag{29}$$

Similarly,

$$\left(\frac{\partial^2 V}{\partial z^2}\right)_o = \frac{V_2 + V_4 - 2V_o}{h^2}$$

Thus, satisfying Laplace's equation at "0",

$$\frac{V_1 + V_2 + V_3 + V_4 - 4V_o}{h^2} + \frac{V_1 - V_3}{2Sh^2} = 0$$

$$\text{or,} \quad V_o = \frac{V_1 + V_2 + V_3 + V_4}{4} + \frac{V_1 - V_3}{8S} \tag{30}$$

Eqn.(30) is valid only when node "0" is away from the axis (i.e. S≠0)

For the node "0" on the axis of symmetry:

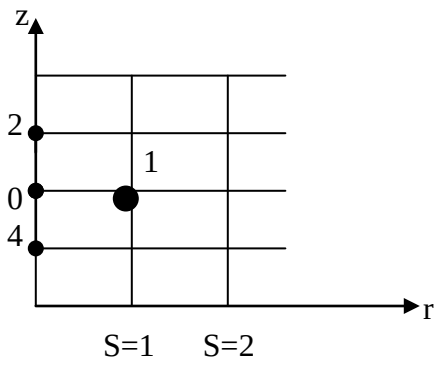

Now, applying L-Hospital's rule

$$\underset{r\to 0}{Lt}\frac{1}{r}\frac{\partial V}{\partial r}=\frac{\partial^2 V}{\partial r^2} \qquad \text{as } \frac{\partial V}{\partial r}\to 0 \qquad \text{when } r\to 0$$

Then, Laplace's eqn. becomes

$$2\frac{\partial^2 V}{\partial r^2}+\frac{\partial^2 V}{\partial z^2}=0 \tag{31}$$

Taylor's series between the nodes 0 and 1,

$$V_1=V_o+h\left(\frac{\partial V}{\partial r}\right)_o+\frac{h^2}{2}\left(\frac{\partial^2 V}{\partial r^2}\right)_o$$

$$\text{or, } \left(\frac{\partial^2 V}{\partial r^2}\right)_o=\frac{2(V_1-V_o)}{h^2} \tag{32}$$

$$\text{as } \left(\frac{\partial V}{\partial r}\right)_o=0$$

$$\text{Again, } \left(\frac{\partial^2 V}{\partial z^2}\right)_o=\frac{V_2+V_4-2V_o}{h^2} \tag{33}$$

Putting in Laplace's Eqn.,

$$\frac{4(V_1 - V_o)}{h} + \frac{V_2 + V_4 - 2V_o}{h^2} = 0$$

or, $$V_o = \frac{4V_1 + V_2 + V_4}{6} \qquad (34)$$

Problem

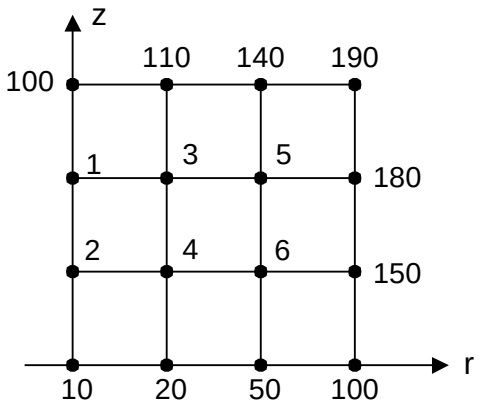

$$V_1 = \frac{4V_3 + V_2 + 100}{6}$$

$$V_2 = \frac{4V_4 + V_1 + 10}{6}$$

$$V_3 = \frac{1}{4}(V_1 + V_4 + V_5 + 110) + \frac{V_5 - V_1}{8 \times 1}, \text{ as } S = 1$$

$$V_4 = \frac{1}{4}(V_2 + V_3 + V_6 + 20) + \frac{V_6 - V_2}{8 \times 1}, \text{ as } S = 1$$

$$V_5 = \frac{1}{4}(V_3 + V_6 + 140 + 180) + \frac{180 - V_3}{8 \times 2}, \text{ as } S = 2$$

$$V_6 = \frac{1}{4}(V_4 + V_5 + 50 + 150) + \frac{150 - V_4}{8 \times 2}, \text{ as } S = 2$$

E) Axi-symmetric System with Unequal Nodal Distance

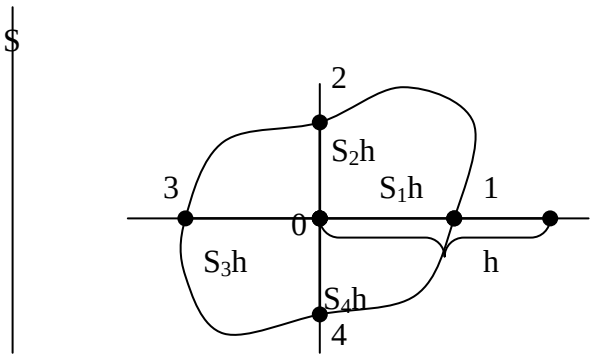

From, Taylor's series expansion,

$$V_1 = V_o + S_1 h\frac{\partial V}{\partial r} + \frac{(S_1 h)^2}{2}\frac{\partial^2 V}{\partial r^2} \tag{35}$$

$$V_3 = V_o - S_3 h\frac{\partial V}{\partial r} + \frac{(S_1 h)^2}{2}\frac{\partial^2 V}{\partial r^2} \tag{36}$$

Now,

$$\frac{V_1}{S_1} = \frac{V_o}{S_1} + h\frac{\partial V}{\partial r} + \frac{S_1 h^2}{2}\frac{\partial^2 V}{\partial r^2}$$

$$\frac{V_3}{S_3} = \frac{V_o}{S_3} - h\frac{\partial V}{\partial r} + \frac{S_3 h^2}{2}\frac{\partial^2 V}{\partial r^2}$$

Hence,

$$\frac{V_1}{S_1} + \frac{V_3}{S_3} = V_o\left(\frac{1}{S_1} + \frac{1}{S_3}\right) + \frac{1}{2}(S_1 + S_3)h^2\frac{\partial^2 V}{\partial r^2}$$

or,

$$\frac{\partial^2 V}{\partial r^2} = \frac{\frac{V_1}{S_1} + \frac{V_3}{S_3} - V_o\left(\frac{1}{S_1} + \frac{1}{S_3}\right)}{\frac{1}{2}(S_1 + S_3)h^2} \tag{37}$$

Again, from Eqns. (35) and (36),

$$\frac{V_1}{S_1^2} = \frac{V_o}{S_1^2} + \frac{h}{S_1}\frac{\partial V}{\partial r} + \frac{h^2}{2}\frac{\partial^2 V}{\partial r^2}$$

$$\frac{V_3}{S_3^2} = \frac{V_o}{S_3^2} - \frac{h}{S_3}\frac{\partial V}{\partial r} + \frac{h^2}{2}\frac{\partial^2 V}{\partial r^2}$$

Thus,

$$\frac{V_1}{S_1^2} - \frac{V_3}{S_3^2} = V_o\left(\frac{1}{S_1^2} - \frac{1}{S_3^2}\right) + h\left(\frac{1}{S_1} + \frac{1}{S_3}\right)\frac{\partial V}{\partial r}$$

or,

$$\frac{\partial V}{\partial r} = \frac{\dfrac{V_1}{S_1^2} - \dfrac{V_3}{S_3^2} - V_o\left(\dfrac{1}{S_1^2} - \dfrac{1}{S_3^2}\right)}{h\left(\dfrac{1}{S_1} + \dfrac{1}{S_3}\right)} \qquad (38)$$

So,

$$\frac{1}{r}\frac{\partial V}{\partial r} = \frac{1}{Sh}\cdot\frac{\partial V}{\partial r} = \frac{\dfrac{V_1}{S_1^2} - \dfrac{V_3}{S_3^2} - V_o\left(\dfrac{1}{S_1^2} - \dfrac{1}{S_3^2}\right)}{Sh^2\,\dfrac{S_1 + S_3}{S_1 S_3}}$$

$$= \frac{V_1\dfrac{S_3}{S_1} - V_3\dfrac{S_1}{S_3}}{(S_1 + S_3)Sh^2} - V_o\frac{S_3 - S_1}{Sh^2 \cdot S_1 S_3} \qquad (39)$$

Following the same procedue as that for $\frac{\partial^2 V}{\partial r^2}$,

$$\frac{\partial^2 V}{\partial z^2} = \frac{\dfrac{V_2}{S_2} + \dfrac{V_4}{S_4} - V_o\left(\dfrac{1}{S_2} + \dfrac{1}{S_4}\right)}{\dfrac{1}{2}(S_2 + S_4)h^2} \qquad (40)$$

Now, putting Eqns. (37), (39) and (40) in Laplace's Eqn.

$$\frac{\frac{V_1}{S_1}+\frac{V_3}{S_3}-V_o\left(\frac{1}{S_1}+\frac{1}{S_3}\right)}{\frac{1}{2}(S_1+S_3)h^2}+\frac{V_1\frac{S_3}{S_1}-V_3\frac{S_1}{S_3}}{(S_1+S_3)Sh^2}-V_o\frac{(S_3-S_1)}{Sh^2S_1S_3}+\frac{\frac{V_2}{S_2}+\frac{V_4}{S_4}-V_o\left(\frac{1}{S_2}+\frac{1}{S_4}\right)}{\frac{1}{2}(S_2+S_4)h^2}=0$$

or,

$$\frac{V_1\frac{2S}{S_1}+V_3\frac{2S}{S_3}}{S_1+S_3}+\frac{V_1\frac{S_3}{S_1}-V_3\frac{S_1}{S_3}}{S_1+S_3}+\frac{V_2\frac{2S}{S_2}+V_4\frac{2S}{S_4}}{S_2+S_4}=V_o\left[\frac{2S}{S_1S_3}+\frac{S_3-S_1}{S_1S_3}+\frac{2S}{S_2S_4}\right]$$

or,

$$V_o=\frac{\frac{1}{S_1+S_3}\left\{\left(\frac{2S+S_3}{S_1}\right)V_1+\frac{2S-S_1}{S_3}V_3\right\}+\frac{2S}{S_2+S_4}\left(\frac{V_2}{S_2}+\frac{V_4}{S_4}\right)}{\frac{2S+S_3-S_1}{S_1S_3}+\frac{2S}{S_2S_4}} \qquad (41)$$

Unequal Nodal Distance for the Node on the Axis

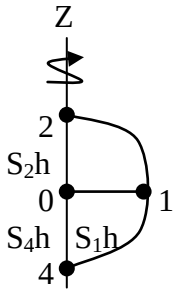

Laplace's Eqn. for the node on the axis:

$$2\frac{\partial^2V}{\partial r^2}+\frac{\partial^2V}{\partial z^2}=0$$

From Taylor's Series expansion between the nodes "0" and "1",

$$V_1=V_o+S_1h\frac{\partial V}{\partial r}+\frac{(S_1h)^2}{2}\frac{\partial^2V}{\partial r^2}$$

or,

$$V_1 - V_o = \frac{(S_1 h)^2}{2}\frac{\partial^2 V}{\partial r^2} \qquad \text{as } \frac{\partial V}{\partial r} = 0 \quad \text{as } r \to 0$$

or.

$$2 \cdot \frac{\partial^2 V}{\partial r^2} = \frac{4(V_1 - V_o)}{(S_1 h)^2} \tag{42}$$

Putting Eqns. (42) and (40) in Laplace's Eqn,

$$\frac{4(V_1 - V_o)}{(S_1 h)^2} + \frac{\dfrac{V_2}{S_2} + \dfrac{V_4}{S_4} - V_o \dfrac{S_2 + S_4}{S_2 S_4}}{\dfrac{1}{2}(S_2 + S_4)h^2} = 0$$

or,

$$\frac{2V_1}{S_1^2} + \frac{1}{S_2 + S_4}\left(\frac{V_2}{S_2} + \frac{V_4}{S_4}\right) = V_o\left(\frac{2}{S_1^2} + \frac{1}{S_2 S_4}\right)$$

or,

$$V_o = \frac{\dfrac{2V_1}{S_1^2} + \dfrac{1}{S_2 + S_4}\left(\dfrac{V_2}{S_2} + \dfrac{V_4}{S_4}\right)}{\dfrac{2}{S_1^2} + \dfrac{1}{S_2 S_4}} \tag{43}$$

Problem

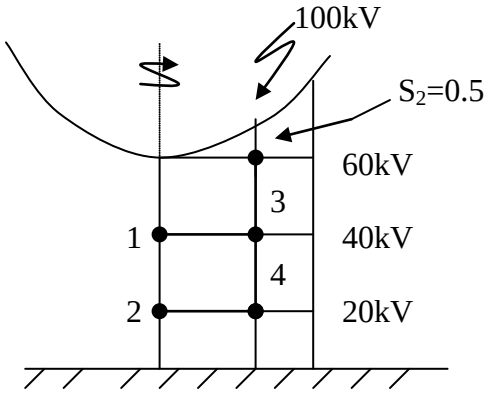

$$V_1 = \frac{1}{6}\left(4V_4 + V_2 + 100\right)$$

$$V_2 = \frac{1}{6}\left(4V_5 + V_1\right)$$

For the node "3"

$$V_o \to V_3,\ V_1 = 60,\ \ V_2 = 100,\ \ V_3 = 100$$

$$S_1 = S_3 = S_4 = 1,\ \ S_2 = 0.5\ \ \&\ \ S = 1$$

Then from Eqn.(41)

$$V_3 = \frac{407 + 1.33V_4}{6}$$

$$V_4 = \frac{1}{4}\left(V_1 + V_3 + V_5 + 40\right) + \frac{40 - V_1}{8}$$

$$V_5 = \frac{1}{4}\left(V_2 + V_4 + 20\right) + \frac{20 - V_2}{8}$$

Calculation of 'S_x' for circular Boundaries:

i)

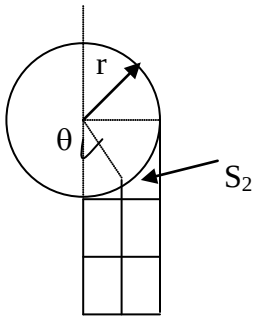

To calculate S_2 :

$$h = \frac{r}{2}$$

$$\sin\theta = \frac{r/2}{r} = \frac{1}{2}$$

$$\text{or, } \theta = 30^o$$

$$\therefore S_2 h = r - r\cos\theta = r\left(1 - 0.866\right)$$

or,

$$S_2 \times \frac{r}{2} = 0.134r$$

or, $S_2 = 0.268$

ii)

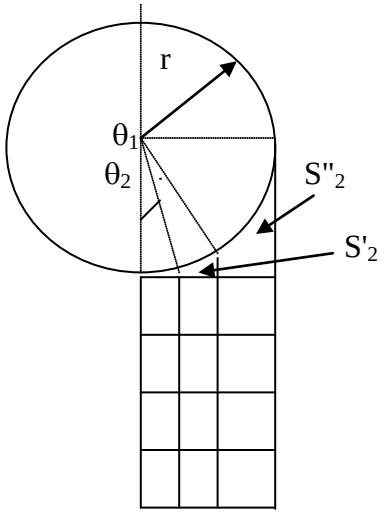

Here, $h = \frac{r}{3}$

$$\sin\theta_1 = \frac{2h}{r} = \frac{2}{3}$$

or, $\theta_1 = 41.81^\circ$

$$\sin\theta_2 = \frac{h}{r} = \frac{1}{3}$$

or, $\theta_2 = 19.47^\circ$

$$S_2' h = r(1 - \cos\theta_2)$$

$$S_2'' h = r(1 - \cos\theta_1)$$

$$\therefore S_2' = 3(1 - \cos 19.47^\circ) = 0.171$$

$$S_2'' = 3(1 - \cos 41.81^\circ) = 0.765$$

F. 2-D Multi-dielectric System

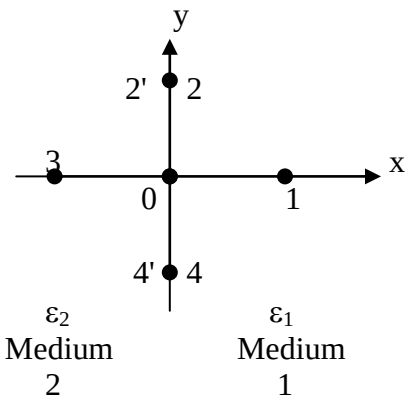

The boundary condition is that the normal component of flux density remains constant in both the sides of the dielectric interface.

i.e, $D_x = D'_x$

or, $\varepsilon_1 E_x = \varepsilon_2 E'_x$

or, $\varepsilon_1 \frac{\partial V}{\partial x} = \varepsilon_2 \frac{\partial V'}{\partial x}$ (44)

Now, nodes 2 and 4 are on the dielectric interface, so the potential and its derivative along y-direction must be same on both sides of the interface.

Moreover, Laplace's equation has to be satisfied on both the sides of interface.

Now, from Taylor's series expansion -

$$V_1 = V_o + h\frac{\partial V}{\partial x} + \frac{h^2}{2}\frac{\partial^2 V}{\partial x^2} \quad (45)$$

$$V_3 = V_o - h\frac{\partial V'}{\partial x} + \frac{h^2}{2}\frac{\partial^2 V'}{\partial x^2} \quad (46)$$

$$V_2 = V_o + h\frac{\partial V}{\partial y} + \frac{h^2}{2}\frac{\partial^2 V}{\partial y^2} \quad (47)$$

$$V_4 = V_o - h\frac{\partial V}{\partial y} + \frac{h^2}{2}\frac{\partial^2 V}{\partial y^2} \tag{48}$$

Now, Laplace's Eqns.-

$$\text{Medium 1}: \frac{\partial^2 V}{\partial x^2} + \frac{\partial^2 V}{\partial y^2} = 0 \tag{49}$$

$$\text{Medium 2}: \frac{\partial^2 V'}{\partial x^2} + \frac{\partial^2 V'}{\partial y^2} = 0 \tag{50}$$

Again, from Eqn.(44)

$$\frac{\partial V'}{\partial x} = \mathrm{K}\frac{\partial V}{\partial x} \tag{51}$$

where, $K = \varepsilon_1 \big/ \varepsilon_2$

From Eqns. (46) & (51)

$$V_3 = V_o - Kh\frac{\partial V}{\partial x} + \frac{h^2}{2}\frac{\partial^2 V'}{\partial x^2} \tag{52}$$

From Eqn.(45),

$$\frac{\partial^2 V}{\partial x^2} = \frac{V_1 - V_o - h\dfrac{\partial V}{\partial x}}{\dfrac{h^2}{2}} \tag{53}$$

From Eqn (52),

$$\frac{\partial^2 V'}{\partial x^2} = \frac{V_3 - V_o + Kh\dfrac{\partial V}{\partial x}}{\dfrac{h^2}{2}} \tag{54}$$

From Eqns.(47) & (48),

$$\frac{\partial^2 V}{\partial y^2} = \frac{V_2 + V_4 - 2V_o}{h^2} = \frac{\partial^2 V'}{\partial y^2} \qquad (55)$$

Thus, from Eqns. (49), (53) and (55),

$$\frac{V_1 - V_o - h\dfrac{\partial V}{\partial x}}{\dfrac{h^2}{2}} + \frac{V_2 + V_4 - 2V_o}{h^2} = 0 \qquad (56)$$

Again from Eqns.(50), (54) & (55),

$$\frac{V_3 - V_o - Kh\dfrac{\partial V}{\partial x}}{\dfrac{h^2}{2}} + \frac{V_2 + V_4 - 2V_o}{h^2} = 0 \qquad (57)$$

From Eqns. (56) and (57),

$$V_o = \frac{\dfrac{2K}{K+1}V_1 + V_2 + \dfrac{2}{K+1}V_3 + V_4}{4} \qquad (58)$$

For single dielectric system, $\mathrm{K} = \dfrac{\varepsilon_1}{\varepsilon_2} = 1.$

Thus from Eqn.(58), $V_o = \dfrac{1}{4}\left(V_1 + V_2 + V_3 + V_4\right)$

which is the same equation as derived earlier for 2-D single-dielectric system.

Problem:

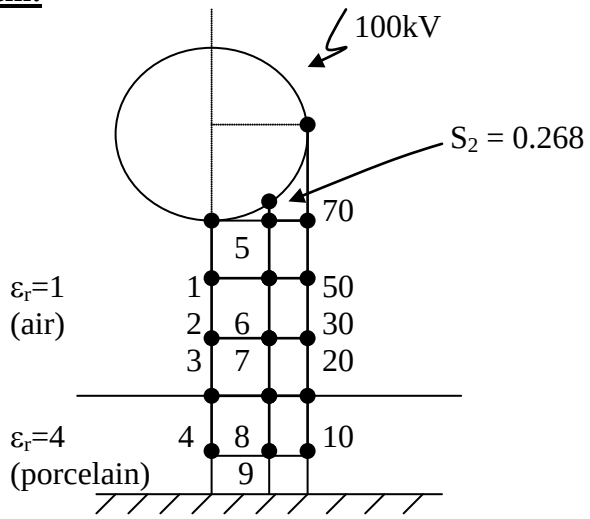

$$K = \frac{\varepsilon_1}{\varepsilon_2} = \frac{1}{4} = 0.25$$

It is a cylindrical system, i.e. 2D arrangement,

$$V_1 = \frac{2V_6 + V_2 + 100}{4}$$

$$V_2 = \frac{2V_7 + V_1 + V_3}{4}$$

For the node "3": $V_o \to V_3$; $V_1 \to V_2$; $V_2 \to V_8$
$V_3 \to V_4$; $V_4 \to V_8$ of eqn.(58)

So, from Eqn.(58),

$$V_3 = \frac{\frac{2 \times 0.25}{1 + 0.25} V_2 + V_8 + \frac{2}{1 + 0.25} V_4 + V_8}{4}$$

Again,

$$V_4 = \frac{2V_9 + V_3}{4}$$

For the node "5", $S_1 = S_3 = S_4 = 1$ and $S_2 = 0.268$

So, from Eqn.(22)

$$V_5 = \frac{\frac{1}{2}\left(\frac{70}{1}+\frac{100}{1}\right)+\frac{1}{1+0.268}\left(\frac{100}{1}+\frac{V_6}{1}\right)}{1+\frac{1}{0.268}}$$

or, $V_5 = 80.18 + 0.166V_6$

Again,

$$V_6 = \frac{1}{4}\left(V_1 + V_7 + 50 + V_5\right)$$

$$V_7 = \frac{1}{4}\left(V_2 + V_6 + V_8 + 30\right)$$

For the node "8" from Eqn. (58),

$$V_8 = \frac{\frac{2\times 0.25}{1+0.25}V_7 + V_3 + \frac{2}{1+0.25}V_9 + 20}{4}$$

and $V_9 = \frac{1}{4}\left(V_4 + V_8 + 10\right)$

Numerical Computation of HV Field by Finite Element Method (FEM)

Introduction

The Finite Element Method (FEM) is a numerical analysis technique to obtain solutions to the differential equations that describe, or approximately describe a wide variety of physical problems ranging from solid, fluid and soil mechanics, to electromagnetism or dynamics. The underlying premise of the FEM is that a complicated region of interest can be sub-divided into a series of smaller sub-regions in which the differential equations are approximately solved. By assembling the set of equations for each sub-region, the behavior over the entire region of interest is determined.

It is difficult to state the exact origin of the FEM, because the basic concepts have evolved over a period of 100 or more years. The term finite element was first coined by Clough in 1960. In the early 1960s, FEM was used for approximate solution of problems in stress analysis, fluid flow, heat transfer, and some other areas. In the late 1960s and early 1970s, application of FEM was extended to much wider variety of engineering problems. Significant advances in mathematical treatments, including the development of new elements, and convergence studies were made in 1970s. Most of the commercial FEM software packages originated in the 1970s and 1980s. The FEM is one of the most important developments in computational methods to occur in the 20th century. The method has evolved from one with applications in structural engineering at the beginning to a widely utilized and richly varied computational approach for many scientific and technological areas at present.

Basics of Finite Element Method

Using the finite element method, the region of interest is discretized into smaller sub-regions called elements as shown in Fig. 15.1, and the solution is determined in terms of discrete values of some primary field variables, e.g. electric potential, at the nodes. The governing equation, e.g. Laplace's or Poisson's equation, is now applied to the domain of a single element. At the element level, the solution to the governing equation is replaced by a continuous function approximating the distribution of the field variable ϕ over the element domain, expressed in terms of the unknown nodal values ϕ_1, ϕ_2 and ϕ_3 of the solution ϕ. A system of equations in terms of ϕ_1, ϕ_2 and ϕ_3 can then be formulated for the element. Once the element equations have been determined, the elements are assembled to form the entire region of interest. Assembly is accomplished using the basic rule that the value of the field variable at a node must be the same for each element that shares that node. The solution ϕ to the problem becomes a piecewise approximation, expressed in terms of the nodal values of ϕ. The assembly procedure results in a system of linear algebraic equations.

Several approaches can be used to transform the physical formulation of the problem to its finite element discrete analogue. If the physical formulation of the problem is known as a differential equation, e.g. Laplace's or Poisson's equation, then the most popular method of its finite element formulation is the Galerkin method. If the physical problem can be formulated as minimization of a functional then variational formulation of the finite element equations is usually used. For problems in high voltage fields, the functional turns out to be the energy stored in the electric field.

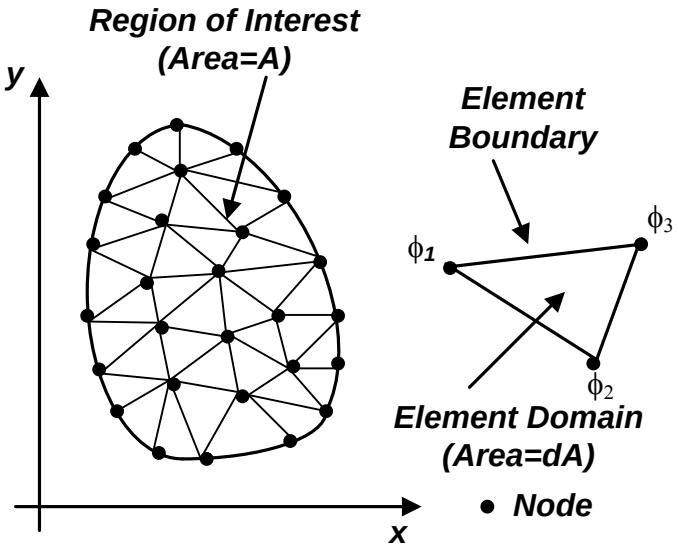

Fig. 15.1 Depiction of Region of interest, element and nodes for FEM formulation

A third and even more versatile approach to deriving element properties is known as the weighted residuals approach. The weighted residuals approach begins with the governing equations of the problem and proceeds without relying on a variational statement. This approach is advantageous because it makes it possible to extend the finite element method to problems where no functional is available.

Procedural Steps in FEM

In general terms, the main steps of the finite element solution procedure are as follows.

1. At the beginning the region of interest is discretized into finite elements.
2. Suitable functions are considered to interpolate the field variables over the element.
3. The matrix equation for the finite element is formed relating the nodal values of the unknown field variables to other physical parameters.
4. Global equation system is formed for the entire region of interest by assembling all the element equations. Element connectivities are used for the assembly process. Boundary conditions, which are not accounted in element equations, are imposed before the solution of equations.
5. The finite element global equation system is solved to get the nodal values of the sought field variables.
6. In many cases additional parameters need to be calculated after the solution of global equation system. For example, in high voltage field problems electric field intensity, electric flux density and charges are of interest in addition to electric potential, which are obtained after solution of the global equation system.

Variational Approach towards FEM Formulation

For high voltage field problems, the principle of minimum potential energy is used in this approach. The principle of minimum potential energy can be stated as: Out of all possible potential functions $\phi(x,y,z)$ the one which minimizes the total potential energy is the potential solution that will satisfy equilibrium, and will be the actual potential due to the applied field forces.

Thus, a potential function that will minimize the functional, i.e potential energy, is desired. Minimization of functionals falls within the field of variational calculus. In most cases an exact function is impossible to determine, necessitating the use of approximate numerical methods. The minimization of potential energy in a finite element formulation is carried out using the energy approach. The finite element method develops the equations from simple element shapes, in which the unknowns of the solution are the potentials at the nodes. The calculus of variations enables the energy equation to be reduced to a set of simultaneous equations with the nodal potentials as the unknown quantities.

FEM Formulation in 2-D System with Single Dielectric Medium

The potential energy in a two-dimensional electric field is given by

$$U_{Total} = \iint_A \frac{1}{2}\varepsilon_o \varepsilon_r \left|\vec{E}\right|^2 .l.dA \qquad \text{…. 15.1}$$

or, $$U_{Total} = \iint_A \frac{1}{2}\varepsilon_o \varepsilon_r \left|-\vec{\nabla}\phi\right|^2 .l.dA \qquad \text{…. 15.2}$$

where, E = electric field intensity, ϕ = electric potential, l = length normal to the area A (usually considered as unity for 2-D field), ε_o = permittivity of free space and ε_r = relative permittivity of dielectric.

The integration of eqn. 15.1 must be carried out over the area A, which is identical to the field region under consideration as shown in Fig. 15.1. Since, this area must be finite, FEM cannot be applied to the problems with "open fields" without modifications.

To apply FEM, the region of interest is to be discretized by so-called finite elements as shown in Fig. 15.1. If a region of interest is divided into elements such that continuity of electric potential between elements is enforced, then the total potential energy is equal to the sum of the individual energies of each element. For N number of elements, the total potential energy can then be stated as:

$$U_{Total} = \sum_{e=1}^{N} U(e) \qquad \text{…. 15.3}$$

To minimize the total potential energy, U, of the entire region of interest, $U(e)$ must be minimized for each element. Seeking a set of nodal potentials for each element will minimize $U(e)$. Observe that the functional, $U(e)$ is a function only of the nodal potentials. Using calculus of variations, an extremization of $U(e)$ occurs when the vector of the first partial derivatives with respect to ϕ is zero.

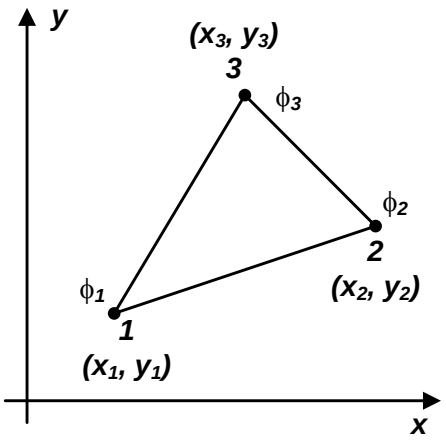

Fig. 15.2 Linear Triangular Element

The simplest 2-D element is the linear triangular element as shown in Fig. 15.2. For this element there are three nodes at the vertices of the triangle, which are numbered around the element in anti-clockwise direction. Electric potential ϕ is assumed to be varying linearly within the element such that

$$\phi = \alpha_1 + \alpha_2 x + \alpha_3 y \quad \text{…. 15.4}$$

Hence, $\vec{E}_x = -\frac{\partial V}{\partial x} = -\alpha_2$ and $\vec{E}_y = -\frac{\partial V}{\partial y} = -\alpha_3$ …. 15.5

Thus, for this element electric field intensity components are constant throughout the element. As a result, this type of element is also known constant stress element (CST).

Now, considering a triangular element as shown in Fig. 15.2

$$\begin{aligned} \phi_1 &= \alpha_1 + \alpha_2 x_1 + \alpha_3 y_1 \\ \phi_2 &= \alpha_1 + \alpha_2 x_2 + \alpha_3 y_2 \\ \phi_3 &= \alpha_1 + \alpha_2 x_3 + \alpha_3 y_3 \end{aligned} \quad \text{…. 15.6}$$

So, from eqn.3.6

$$\alpha_2 = \frac{\begin{vmatrix} 1 & \phi_1 & y_1 \\ 1 & \phi_2 & y_2 \\ 1 & \phi_3 & y_3 \end{vmatrix}}{\begin{vmatrix} 1 & x_1 & y_1 \\ 1 & x_2 & y_2 \\ 1 & x_3 & y_3 \end{vmatrix}}$$

or, $\alpha_2 = \frac{1}{D}\left[\phi_1(y_2 - y_3) + \phi_2(y_3 - y_1) + \phi_3(y_1 - y_2)\right]$ …. 15.7

where, $D = (x_2 y_3 - x_3 y_2) + (x_3 y_1 - x_1 y_3) + (x_1 y_2 - x_2 y_1)$ …. 15.8

= 2 times the area of the triangle

Similarly, $\alpha_3 = \frac{1}{D}\left[\phi_1(x_3 - x_2) + \phi_2(x_1 - x_3) + \phi_3(x_2 - x_1)\right]$ …. 15.9

The magnitude of the electric field intensity within an element *T*,

$$\left|\vec{E}_T\right| = \sqrt{\left|E_x^2\right| + \left|E_y^2\right|} = \sqrt{\alpha_2^2 + \alpha_3^2} \quad \text{…. 15.10}$$

Hence, the electric potential energy in an element *T*

$$U_T = \frac{1}{2}\varepsilon_o \varepsilon_r \left|\vec{E}_T\right|^2 A.l = \frac{1}{2}\varepsilon_o \varepsilon_r A.l.\left(\alpha_2^2 + \alpha_3^2\right) \quad \text{…. 15.11}$$

For electric potential energy in an element to be minimum,

$$\frac{\partial U_T}{\partial \phi_1} = \frac{1}{2}\varepsilon_o \varepsilon_r A.l.2\left(\alpha_2 \frac{\partial \alpha_2}{\partial \phi_1} + \alpha_3 \frac{\partial \alpha_3}{\partial \phi_1}\right) = 0 \quad \text{…. 15.12}$$

Eqn. 15.12 is to be applied to every node where the unknown potential is to be determined. It may be noted here that the node under consideration may belong to more than one element. Then Eqn. 15.12 is to be applied for all such elements considering the node under consideration as *node-1* and the other two nodes of the element being *node-2* and *node-3* taken in anti-clockwise direction.

Now, $\frac{\partial \alpha_2}{\partial \phi_1} = \frac{y_2 - y_3}{D}$, $\frac{\partial \alpha_3}{\partial \phi_1} = \frac{x_3 - x_2}{D}$ and *A=D/2*

So, from eqn. 15.12

$$\frac{1}{2}\varepsilon_o\varepsilon_r\frac{D}{2}.l.2\left[\alpha_2\frac{y_2-y_3}{D}+\alpha_3\frac{x_3-x_2}{D}\right]=0$$

$$or,\quad \frac{1}{2}\varepsilon_o\varepsilon_r.l.\left[\alpha_2(y_2-y_3)+\alpha_3(x_3-x_2)\right]=0 \qquad \text{…. 15.13}$$

Hence, from eqns. 15.7, 15.9 and 15.13

$$\frac{\varepsilon_o\varepsilon_r l}{2D}\left[\{\phi_1(y_2-y_3)+\phi_2(y_3-y_1)+\phi_3(y_1-y_2)\}(y_2-y_3)\right.$$
$$\left.+\{\phi_1(x_3-x_2)+\phi_2(x_1-x_3)+\phi_3(x_2-x_1)\}(x_3-x_2)\right]=0 \qquad \text{…. 15.14a}$$

or,
$$\frac{\varepsilon_r}{D}\left[\phi_1\left\{(x_3-x_2)^2+(y_2-y_3)^2\right\}+\phi_2\{(x_3-x_2)(x_1-x_3)+(y_2-y_3)(y_3-y_1)\}\right.$$
$$\left.+\phi_3\{(x_3-x_2)(x_2-x_1)+(y_2-y_3)(y_1-y_2)\}\right]=0 \qquad \text{…. 15.14b}$$

or,
$$K_{1T}\phi_1+K_{2T}\phi_2+K_{3T}\phi_3=0 \qquad \text{…. 15.15}$$

where,
$$K_{1T}=\frac{\varepsilon_{rT}}{D_T}\left[(x_{3T}-x_{2T})^2+(y_{2T}-y_{3T})^2\right]$$

$$K_{2T}=\frac{\varepsilon_{rT}}{D_T}\left[(x_{3T}-x_{2T})(x_{1T}-x_{3T})+(y_{2T}-y_{3T})(y_{3T}-y_{1T})\right] \qquad \text{…. 15.16}$$

$$K_{3T}=\frac{\varepsilon_{rT}}{D_T}\left[(x_{3T}-x_{2T})(x_{2T}-x_{1T})+(y_{2T}-y_{3T})(y_{1T}-y_{2T})\right]$$

In eqn. 15.16, subscript T denotes the element number, D_T is twice the area of the element as given by eqn. 15.8 and ε_{rT} is the permittivity of the dielectric within the element.

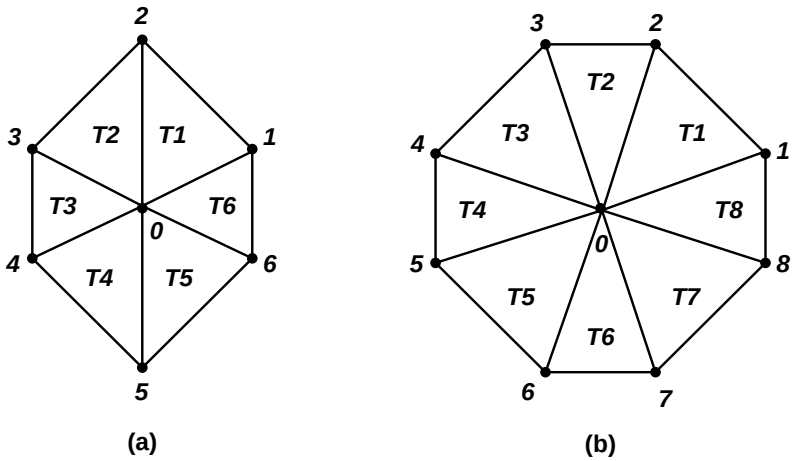

Fig. 15.3 Nodal connectivity – a) 6-element (Hexagonal), b) 8-element (Octagonal)

Discretization using triangular elements is usually done is such a way that one particular node is connected to either 6 other nodes in hexagonal connectivity as shown in Fig. 15.3(a) or to 8 other nodes in octagonal connectivity as shown in Fig. 15.3(b). For hexagonal connectivity, an equation may be formed involving potentials of all the six nodes surrounding the node "*0*" applying eqn. 15.15. In such case, for every element, *node-0* of Fig. 15.3 is considered to be *node-1* of eqn. 15.15 and the other two nodes are considered to be *node-2* and *node-3* in anti-clockwise direction. Application of eqn. 15.15 thus results in six simultaneous linear equations, the summation of which may be represented as follows.

$$F_1\phi_1 + F_2\phi_2 + F_3\phi_3 + F_4\phi_4 + F_5\phi_5 + F_6\phi_6 + F_0\phi_0 = 0 \quad \text{…. 15.17}$$

where,

$$F_1 = K_{2(T1)} + K_{3(T6)}$$
$$F_2 = K_{2(T2)} + K_{3(T1)}$$
$$F_3 = K_{2(T3)} + K_{3(T2)}$$
$$F_4 = K_{2(T4)} + K_{3(T3)} \quad \text{…. 15.18}$$
$$F_5 = K_{2(T5)} + K_{3(T4)}$$
$$F_6 = K_{2(T6)} + K_{3(T5)}$$
$$\text{and } F_0 = \sum_{T=1}^{6} K_{1T}$$

Application of eqn. 15.17 to all the nodes having unknown potential will generate the FEM system of simultaneous linear equations, which needs to be solved for determining the node potentials. Eqns. 15.17 and 15.18 could be suitably modified for octagonal nodal connectivity. Here, it may also be noted that FEM formulation as described above automatically takes into account the unequal elemental sizes as the coefficients as in eqn. 15.18 are all computed in terms of nodal coordinates that may have any numerical values.

FEM Formulation in 2-D System with Multi-Dielectric Media

For computing electric field in a multi-dielectric media, triangular elements are so positioned that any given triangular element comprises only one dielectric medium. In other words, a set of nodal points are to be placed on the interface between two dielectrics as shown in Fig. 15.4. Hence, the coefficients K_{1T}, K_{2T} and K_{3T} for any node are to be calculated depending on its nodal position (i.e. *1*, *2* or *3*) in an element considering the proper value of ε_r.

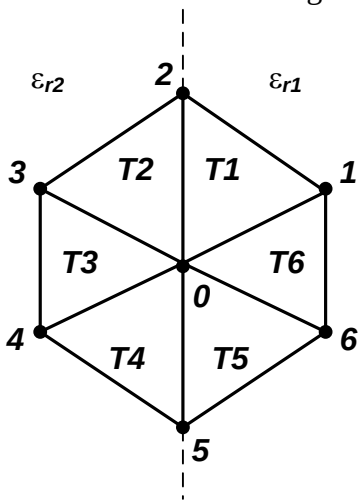

Fig. 15.4 Elemental discretization for multi-dielectric media

While applying eqn. 15.17 for the nodal connectivity shown in Fig. 15.4, the following modifications need to be made for F_2, F_5 and F_0 keeping the others unchanged.

$$F_2 = K_{2(T2)} + K_{3(T1)} \;,\; F_5 = K_{2(T5)} + K_{3(T4)} \text{ and } F_0 = \sum_{T=1}^{6} K_{1T}$$

where,

$$K_{2(T2)} = \frac{\varepsilon_{r2}}{D_{T2}}\left[(x_3 - x_2)(x_0 - x_3) + (y_2 - y_3)(y_3 - y_0)\right]$$

$$K_{3(T1)} = \frac{\varepsilon_{r1}}{D_{T1}}\left[(x_2 - x_1)(x_1 - x_0) + (y_1 - y_2)(y_0 - y_1)\right]$$

$$K_{2(T5)} = \frac{\varepsilon_{r1}}{D_{T5}}\left[(x_6 - x_5)(x_0 - x_6) + (y_5 - y_6)(y_6 - y_0)\right]$$

$$K_{3(T4)} = \frac{\varepsilon_{r2}}{D_{T4}}\left[(x_5 - x_4)(x_4 - x_0) + (y_4 - y_5)(y_0 - y_4)\right]$$

For the computation of F_0, K_{1T} is to be calculated considering ε_{r1} for the elements *1, 5* and *6* and considering ε_{r2} for the elements *2, 3* and *4*, using eqn. 15.16. For example, for elements *T3* and *T6*, respectively, the expressions for K_{1T} will be as follows.

$$K_{1(T3)} = \frac{\varepsilon_{r2}}{D_{T3}}\left[(x_4 - x_3)^2 + (y_3 - y_4)^2\right]$$

and $$K_{1(T6)} = \frac{\varepsilon_{r1}}{D_{T6}}\left[(x_1 - x_6)^2 + (y_6 - y_1)^2\right]$$

Here, it may be noted that no separate formulation is required for multi-dielectric media in FEM in contrast to FDM.

FEM Formulation in Axi-symmetric System

As already discussed, electric potential energy in a triangular element is

$$U_e = \frac{1}{2}\varepsilon_o\varepsilon_r\left|\vec{E}\right|^2.A.l \qquad \text{…. 15.19}$$

where, (*A.l*) is the volume of the element.

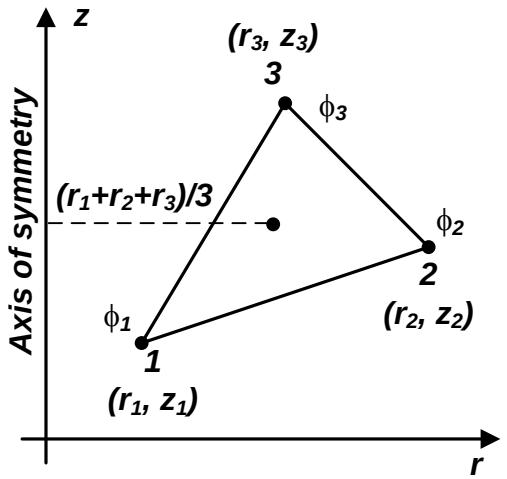

Fig. 15.5 Triangular element for axi-symmetric formulation

For axi-symmetric system, this volume is created due to the rotation of a triangular element around the axis of symmetry. The area of the triangle being *A*, *l* should then be the mean length of rotation, i.e. 2π times the radial distance of the centroid of the triangle.

So, $$l = 2\pi\frac{(r_1 + r_2 + r_3)}{3} \qquad \text{…. 15.20}$$

Putting this expression for *l* in eqn. 15.14b

$$\frac{\varepsilon_o \varepsilon_r}{2D} \cdot \frac{2\pi(r_1 + r_2 + r_3)}{3} \Big[\phi_1 \{(r_3 - r_2)^2 + (z_2 - z_3)^2\} + \phi_2 \{(r_3 - r_2)(r_1 - r_3) + (z_2 - z_3)(z_3 - z_1)\} + \phi_3 \{(r_3 - r_2)(r_2 - r_1) + (z_2 - z_3)(z_1 - z_2)\}\Big] = 0 \quad \ldots \text{ 15.21}$$

So, from eqn. 15.21 in axi-symmetric system

$$K_{1T}\phi_1 + K_{2T}\phi_2 + K_{3T}\phi_3 = 0$$

$$K_{1T} = \frac{R\varepsilon_{rT}}{D_T}\left[(r_{3T} - r_{2T})^2 + (z_{2T} - z_{3T})^2\right]$$

where, $$K_{2T} = \frac{R\varepsilon_{rT}}{D_T}\left[(r_{3T} - r_{2T})(r_{1T} - r_{3T}) + (z_{2T} - z_{3T})(z_{3T} - z_{1T})\right] \quad \ldots. \text{ 15.22}$$

$$K_{3T} = \frac{R\varepsilon_{rT}}{D_T}\left[(r_{3T} - r_{2T})(r_{2T} - r_{1T}) + (z_{2T} - z_{3T})(z_{1T} - z_{2T})\right]$$

and $$R = (r_1 + r_2 + r_3)$$

For axi-symmetric system with multi-dielectric media, the modifications to be brought in are the same as those described for two-dimensional formulation discussed in section 15.4.2.

Numerical Computation of HV Field by Charge Simulation Method (CSM)

Introduction

The principle of FDM and FEM is to provide the entire region of interest into a large number of sub-regions, and solve for unknown potentials a set of coupled simultaneous linear equations which approximate Laplace's or Poisson's equation. Compared to these two methods, only boundary surfaces, i.e. electrode surfaces and dielectric interfaces, are subdivided and charges are taken as unknowns in CSM. It follows, firstly, that the amount of human time and effort needed for subdivision is greatly reduced in CSM. Secondly, the electric field strength can be given explicitly in CSM without any numerical differentiation of the potential, which results in significant reduction in error. The second characteristic is very important because the field strength is usually more important for the design of an insulating system than electric potential.
The earlier attempts for numerical field solutions employing CSM were reported by Loeb et a1 in 1950 and then by Abou-Seada and Nasser (IEEE-PAS, 1969, pp1802-1814). Subsequently, in a comprehensive paper Singer, Steinbigler and Weiss presented the details of CSM (IEEE-PAS, 1974, pp1660-1668). Since then many refinements to the original method have been proposed and CSM has evolved into a very powerful and efficient tool for computing electric fields in HV equipments. CSM is very simple and applicable to systems having more than one dielectric medium. This method is also suitable for 3-D fields with or without symmetry.

CSM Formulation for Single Dielectric Medium

The basic principle of conventional CSM is very simple. For the calculation of electric fields, the distributed charges on the surface of the electrode are replaced by N number of fictitious charges placed inside the electrode as shown in Fig.16.1. The fictitious charges are placed inside the electrode to avoid singularity problem. In general, the fictitious charges are to be always placed outside the region of interest (ROI), as the field is ideally required to be determined at all the points within the ROI. If the fictitious charges are placed within the ROI, then at the location of the fictitious charges singularity arises because at these points the distance between the charge and the point at which the field solution is required becomes zero.

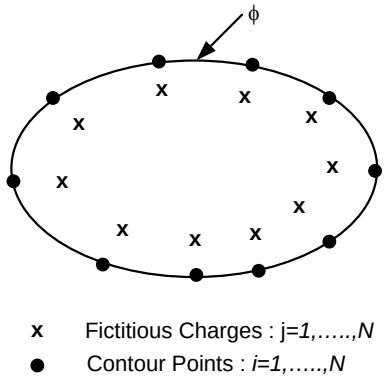

Fig. 16.1 Fictitious charges and contour points for CSM formulation in single dielectric medium

The types and positions of these fictitious charges are predetermined, i.e. user-defined, but their magnitudes are unknown. In order to determine their magnitude some collocation points, which are called contour points, are selected on the surface of electrode. In the

conventional CSM the number of contour points is chosen to be equal to the number of fictitious charges. Then it is required that at any one of these contour points the potential resulting from superposition of effects all the fictitious charges is equal to the known electrode potential. Let, Q_j be the *jth* fictitious charge and ϕ be the known potential of the electrode. Then according to the superposition principle

$$\sum_{j=1}^{N} P_{ij} Q_j = \phi \qquad \text{…. 16.1}$$

where, P_{ij} is the potential coefficient, i.e. the potential at the point *i* due to a unit charge at the location *j*, which can be evaluated analytically for different types of fictitious charges by solving Laplace's equation. When Eqn. 16.1 is applied to *N* no. of contour points, it leads to the following system of *N* linear equations for N unknown fictitious charges

$$\begin{aligned}
&P_{11}Q_1 + P_{12}Q_2 + ... + P_{1j}Q_j + ... + P_{1N}Q_N = \phi \\
&P_{21}Q_1 + P_{22}Q_2 + ... + P_{2j}Q_j + ... + P_{2N}Q_N = \phi \\
&. \\
&P_{i1}Q_1 + P_{i2}Q_2 + ... + P_{ij}Q_j + ... + P_{iN}Q_N = \phi \\
&. \\
&P_{N1}Q_1 + P_{N2}Q_2 + ... + P_{Nj}Q_j + ... + P_{NN}Q_N = \phi
\end{aligned} \qquad \text{…. 16.2}$$

In matrix form, Eqn 16.2 can be written as

$$\begin{bmatrix}
P_{11} & P_{12} ..... P_{1j} ..... P_{1N} \\
P_{21} & P_{22} ..... P_{2j} ..... P_{2N} \\
. & \\
P_{i1} & P_{i2} ..... P_{ij} ..... P_{iN} \\
. & \\
P_{N1} & P_{N2} ..... P_{Nj} ..... P_{NN}
\end{bmatrix}_{N\times N}
\begin{bmatrix} Q_1 \\ Q_2 \\ . \\ Q_i \\ . \\ Q_N \end{bmatrix}_{N\times 1}
= [\phi]_{N\times 1} \qquad \text{…. 16.3}$$

where, [*P*] = potential coefficient matrix, [ϕ] = column vector of known potential of contour points.

Eqn. 16.3 is solved for the unknown fictitious charges. As soon as the required fictitious charge system is determined, the potential and the field intensity at any point within the ROI can be calculated. While the potential is found by Eqn. 16.1, the electric field intensities are calculated by superposition of all the stress vector components. For example, in Cartesian co-ordinate system, the three superimposed field components at any point *i* are given as follows.

$$E_{x,i} = -\sum_{j=1}^{N} \frac{\partial P_{ij}}{\partial x} Q_j = -\sum_{j=1}^{N} F_{x,ij} Q_j \qquad \text{…. 16.4}$$

$$E_{y,i} = -\sum_{j=1}^{N} \frac{\partial P_{ij}}{\partial y} Q_j = -\sum_{j=1}^{N} F_{y,ij} Q_j \qquad \text{…. 16.5}$$

and $$E_{z,i} = -\sum_{j=1}^{N} \frac{\partial P_{ij}}{\partial z} Q_j = -\sum_{j=1}^{N} F_{z,ij} Q_j \qquad \text{…. 16.6}$$

where, $F_{x,ij}$, $F_{y,ij}$ and $F_{z,ij}$ are the electric field intensity coefficients in the *x*, *y* and *z* directions, respectively, i.e. the components in the *x*, *y* and *z* directions, respectively, of electric field intensity at the point *i* for a unit charge at the location *j*.

In many cases the effect of the ground plane is to be considered for electric field calculation. This plane can be taken into account by the introduction of image charge.

Formulation for Floating Potential Electrodes

Floating potential conductors are often present in high voltage system, the most common example being condenser bushings. If floating electrodes are present, whose potentials are constant but unknown, then the boundary condition that is imposed for field computation is given below.

$$\phi_{i+1} - \phi_i = 0, \quad for \;\; i = 1,...., N-1 \qquad \ldots. 16.7$$

Moreover, a supplementary condition is included such that the sum of fictitious charges for each floating electrode is zero.

Then the system of equation that is obtained will be as follows

$$\begin{bmatrix} 1 & 1 & ..... & 1 & ..... & 1 \\ (P_{21}-P_{11}) & (P_{22}-P_{12}) & ..... & (P_{2j}-P_{1j}) & ..... & (P_{2N}-P_{1N}) \\ (P_{31}-P_{21}) & (P_{32}-P_{22}) & ..... & (P_{3j}-P_{2j}) & ..... & (P_{3N}-P_{2N}) \\ . & & & & & \\ (P_{(i+1)1}-P_{i1}) & (P_{(i+1)2}-P_{i2}) & ..... & (P_{(i+1)j}-P_{ij}) & ..... & (P_{(i+1)N}-P_{iN}) \\ . & & & & & \\ (P_{N1}-P_{(N-1)1}) & (P_{N2}-P_{(N-1)2}) & ..... & (P_{Nj}-P_{(N-1)j}) & ..... & (P_{NN}-P_{(N-1)N}) \end{bmatrix}_{N\times N} \begin{bmatrix} Q_1 \\ Q_2 \\ . \\ Q_i \\ . \\ Q_N \end{bmatrix}_{N\times 1} = [0]_{N\times 1} \qquad \ldots 16.8$$

If the floating electrode has a net charge, then the supplementary condition is included such that the sum of its fictitious charges is equal to the known net charge value (Q_E). In Eqn. 16.8 the first row is then modified as follows

$$Q_1 + Q_2 + ... + Q_j + ... + Q_N = Q_E \qquad \ldots. 16.9$$

CSM Formulation for Multi-Dielectric Media

The field computation for a multi-dielectric system is somewhat complicated due to the fact that the dipoles are realigned in dielectric media under the influence of the applied voltage. Such realignment of dipoles produces a net surface charge on the dielectric interface. Thus in addition to the electrodes, each dielectric interface needs to be simulated by fictitious charges. Here, it is important to note that the dielectric boundary does not correspond to an equipotential surface. Moreover, it must be possible to calculate the electric field on both sides of the dielectric boundary.

It has been mentioned earlier that the fictitious charges should be outside the ROI. In the case of electrodes this has been achieved by placing the charges within the electrodes. But, for dielectric-dielectric interface, both the sides are within the ROI. Hence, any fictitious charge placed on either side of the interface would cause singularity problem. This issue is solved by placing two charges for every contour point on the dielectric –dielectric interface. For solving the field within the dielectric-A, the set of charges placed within dielectric-B are considered and vice-versa.

In the simple example shown in Fig. 16.2, there are N_1 number of charges and contour points to simulate the electrode, of which N_A are on the side of dielectric-*A* and $(N_1\text{-}N_A)$ are on the side of dielectric-*B*. These N_1 charges are valid for field calculation in both the dielectrics. At the dielectric interface there are N_2 contour points sequentially numbered from $(N_1+1,\ldots,N_1+N_2)$, with N_2 charges $(N_1+1,\ldots,N_1+N_2)$ in dielectric-*A* valid for dielectric-*B* and N_2 charges $(N_1+N_2+1,\ldots, N_1+2N_2)$ in dielectric-*B* valid for dielectric-*A*. Altogether there are (N_1+N_2) number of contour points and $(N_1+ 2N_2)$ number of fictitious charges.

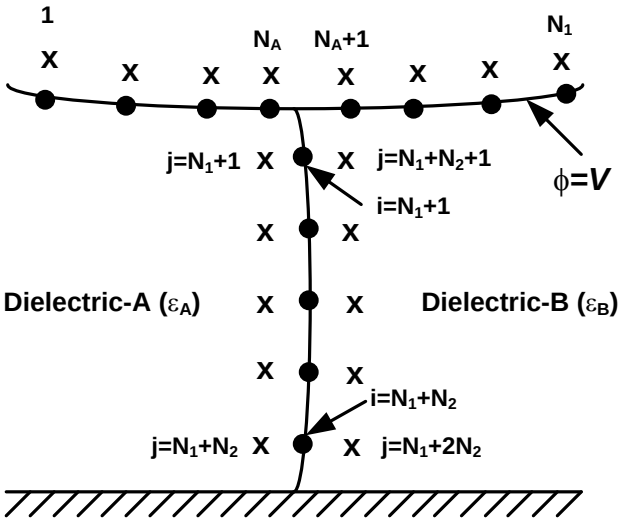

Fig. 16.2 Arrangement of fictitious charges for multi-dielectric media

In order to determine the fictitious charges, a system of equations is formulated by imposing the following boundary conditions.

i) At each contour point on the electrode surface the potential must be equal to the known electrode potential. This condition is also known as Dirichlet's condition on the electrode surface.

ii) At each contour point on the dielectric interface, the potential and the normal component of flux density must be same when computed from either side of the boundary.

Thus the application of the first boundary condition to contour points *1* to N_1 yields the following equations.

$$\sum_{j=1}^{N_1} P_{ij} Q_j + \sum_{j=N_1+N_2+1}^{N_1+2N_2} P_{ij} Q_j = V \qquad .....i = 1, N_A \qquad \text{…. 16.10}$$

and

$$\sum_{j=1}^{N_1} P_{ij} Q_j + \sum_{j=N_1+1}^{N_1+N_2} P_{ij} Q_j = V \qquad .....i = N_A + 1, N_1 \qquad \text{…. 16.11}$$

Again the application of the second boundary condition for potential and normal flux density to contour points N_1+1 to N_1+N_2 on the dielectric interface results into the following equations.

From potential continuity condition:

$$\sum_{j=N_1+1}^{N_1+N_2} P_{ij} Q_j - \sum_{j=N_1+N_2+1}^{N_1+N_2} P_{ij} Q_j = 0 \qquad .....i = N_1 + 1, N_1 + N_2 \qquad \text{…. 16.12}$$

From continuity condition of normal flux density D_n :

$$D_{nA}(i) - D_{nB}(i) = 0 \qquad .....i = N_1 + 1, N_1 + N_2 \qquad \text{…. 16.13}$$

Eqn. 16.13 can be expanded as follows.

$$(\varepsilon_A - \varepsilon_B) \sum_{j=1}^{N_1} F_{n,ij} Q_j - \varepsilon_B \sum_{j=N_1+1}^{N_1+N_2} F_{n,ij} Q_j + \varepsilon_A \sum_{j=N_1+N_2+1}^{N_1+2N_2} F_{n,ij} Q_j = 0 .....i = N_1 + 1, N_1 + N_2 \qquad \text{…. 16.14}$$

where, $F_{n,ij}$ is the field coefficient in the normal direction to the dielectric boundary at the respective contour point and ε_A & ε_B are the permittivities of dielectric *A* and *B*, respectively. Eqns. 16.10 to 16.14 are solved to determine the unknown fictitious charges. These equations can be presented in matrix form as detailed below.

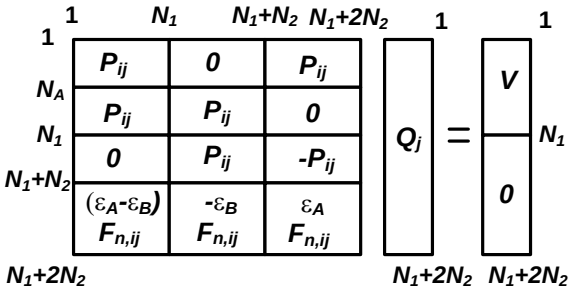

Types of Fictitious Charges

The successful application of the CSM requires a proper choice of the types of fictitious charges. Point and line charges of infinite and semi-infinite lengths were used in the initial works on this method. Steinbigler et al introduced ring charges and finite length line charges. Subsequently, a large variety of different charge configurations have been proposed. These other types of charge configurations include elliptic cylindrical charge, axi-spheroidal charge, plane sheet charge, disk charge, ring segment charge, volume charges, shell and annular plate charges as well as variable density line charge.

In general, the choice of type of fictitious charge to be used depends upon the complexity of the physical system and the available computational facilities. The potential and field coefficients for point and line charges are given by simple expressions and require very small computation time. For complex charge configuration, such coefficients may have to be computed numerically. On the other hand, a smaller number of charges may be used if complex charge configurations are employed, which reduces the overall memory requirement and computation time. In practice, most of the HV systems can be successfully simulated by using point, line and ring charges or a suitable combination of these charges.

Accuracy Criteria

If the fictitious charges completely satisfy the boundary conditions, then these charges give the correct field distribution not only on the boundary but also everywhere outside it. But in the CSM, the fictitious charges are required to satisfy the boundary conditions only at a selected number of contour points. Again the number of contour points is kept small in order to reduce the computer memory and computation time. Hence, it is essential to ensure that the simulation is accurate. To determine the simulation accuracy, the following criteria can be used.

i) The “potential error” on the electrode can be computed at a number of control points on the electrode surface between two contour points. The potential error is defined as the difference between the known potential of the electrode and the computed potential at the control point.

ii) Compared to the potential error the “deviation angle” on the electrode surface is a more sensitive indicator of the simulation accuracy. The deviation angle is defined as the angular deviation of the electric field intensity vector at the control point on the electrode surface from the direction of the normal to its surface.

Another very severe accuracy criterion is to check that the derivative of the potential gradient perpendicular to the electrode surface at the control point divided by the gradient itself is equal to the curvature at this point or not. This is especially applicable for simulation of areas of the electrode with a small radius of curvature.

iii) In multi-dielectric systems the "potential discrepancy" can be computed at a number of control points for each dielectric interface. The potential discrepancy is defined as the difference in the value of potential at the control point when computed from both the sides of the dielectric interface. Alternatively, the discrepancy in the tangential electric stress at the control points on the dielectric interface can also be computed. Another criterion for checking the simulation accuracy is to compute the discrepancy in the normal flux density at the control point on the dielectric interface.

For a good simulation all the above discrepancies should be small.

Factors Affecting Simulation Accuracy

The simulation accuracy in the CSM depends upon the types and number of fictitious charges as well as locations of fictitious charges and contour points. In general, the simulation error can be reduced by increasing the number of charges. However, it has been found that increasing the number of fictitious charges beyond a certain limit does not necessarily improve the simulation accuracy. Generally, the "assignment factor" (λ) defined as the ratio of the distance between a contour point and the corresponding charge (*a2*) to the distance between two successive contour points (*a1*), as shown in Fig. 16.14, considerably affects the simulation accuracy. Steinbigler et al (IEEE-PAS, 1974) suggested that this factor should be between 1.0 and 2.0. Several others suggest a range of $0.7<\lambda<1.5$.

In a good simulation, potential error values as low as 0.001% are possible. However, for sharp corners and thin electrodes, such low values are difficult to achieve. Since the electric field intensity error is an order of magnitude higher than the potential error, potential error values of about 0.1% are considered reasonable. For multi-dielectric systems, if the dielectric boundary has a complex shape, comparatively large potential discrepancy values of the order of 1% are usually acceptable.

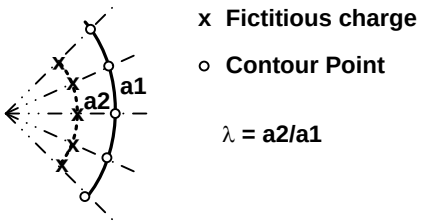

Fig. 16.14 Definition of assignment factor

Manufacturing tolerances of the conductors define the practical limit for the accuracy of the simulation of electrodes. In the same way, the accuracy of the determination of dielectric constants of the involved media puts the practical limit on the accuracy of the simulation of dielectrics.

Solution of System of Equations in CSM

The application of CSM for numerical field calculation involves solutions of linear systems of equations as explained in earlier sections. In the conventional CSM, for a single dielectric case, the matrix of the linear system of equations to be solved is in general asymmetrical without a zero term as detailed in section 16.2. In such cases, the equations could be solved using the Gaussian elimination technique with or without partial or complete pivoting.

In multi-dielectric systems, the matrix of systems of equations to be solved is rather heterogeneous and is not symmetrical as detailed in section 16.3. Due to bad conditioning of the matrix, it is preferable to solve it by using a direct method, e.g. Gaussian elimination technique, to avoid non-convergence problem, which may arise in the case of iterative methods. However, for complicated problems the size of the matrix becomes too large. In such cases, iterative methods such as Gauss-Seidel method or the successive over relaxation method with varying values of acceleration factor have also been found to be successful.

Comparison of CSM with FEM

Both the FEM and CSM are extensively used for numerical calculation of electric field in high voltage engineering.

In FEM, the entire region of interest is subdivided into a large number of sub-regions and a set of coupled simultaneous linear equations, which minimize the electrostatic energy in the field region, are solved for unknown node potentials. On the other hand, in CSM only boundary surface, i.e. electrode surface and dielectric interfaces, are subdivided with fictitious charges which are taken as unknowns. Therefore, it follows that the amount of time and effort needed for subdivision is greatly reduced in CSM. Moreover, the system of equations thus obtained by discretization is of smaller dimension in CSM.

FEM is useful for two-dimensional and also three-dimensional systems with or without symmetry and is advantageous for the calculation of fields where the boundaries have complicated shapes. However, for computing field distribution at a large distance from the HV electrodes by FEM, a large number of nodes and hence excessive computation time and computer memory space are required. Thus, FEM is more suited for problems where the space is bounded. On the contrary, application of CSM is easy with high precision for field problems having infinity extended unbounded region and for relatively simple boundary geometries but not so for fields with complex electrode configurations.

In FEM exact field intensity at any point cannot be obtained. Instead average field intensity between two nodes is to be calculated from the known values of node potentials or numerical differentiation of the potential has to be done. But, in CSM the electric field intensity can be obtained explicitly with the fictitious charges without resorting to numerical differentiation of the potential, which results in significant reduction in error. With proper positioning of the fictitious charges and the contour points and with the optimum number of fictitious charges, the potential and stress errors can be made less than 0.01% and 0.1%, respectively, in CSM. Though FEM is more suited for multiple dielectric problems, CSM can also be effectively employed for fields with many dielectrics.

A major disadvantage of CSM was that the electric field is difficult to calculate in systems having very thin electrodes because fictitious charges have to be placed within the electrodes. However, this disadvantage is obviated by the application of Region Oriented CSM in recent years. Further, CSM is usually, more accurate and less trouble-some in computing Laplacian fields than FEM, but is difficult to use for non-Laplacian fields, e.g. Poissonian fields. However, CSM with complex fictitious charges has been developed for calculating Poissonian field including volume and surface resistance providing very accurate results. Again, CSM is not suited for specific fields containing space charges where FEM can be employed very effectively. But, now-a-days suitable boundary conditions have been postulated for use in connection with CSM for computing spacer surface fields in compact GIS as modified by the charges accumulated on the spacer surface.

Sphere or Cylinder in Uniform External Field

Introduction

Conducting and dielectric components are integral parts of any electrical equipment. If the size of the conducting or dielectric object is very small compared to dimensions of the field region where the object is located, then the object contributes to the field only in the domain near the object. In many cases, such objects are present as stray bodies in high voltage insulation arrangement. As practical examples one may cite a small piece of conductor or dielectric floating in liquid insulation of large volume in transformers, metallic dust particles floating in gaseous insulation within gas insulated system etc. It is important to understand how the presence of a conducting or dielectric object modifies the external field in the vicinity of the object, because any enhancement of electric field intensity due to the conducting or dielectric object may lead to unwanted discharge or in the worst case failure of the insulation system.

If it is assumed that the source charges (in practical arrangement, the electrodes or conductors with specific potentials) that produce the external field is located far away from the object under consideration, then they are unaffected by the presence of the object. Consequently, the field due to the source charges may be considered to be uniform at the location of the object. If the object is such that its shape is defined by well known mathematical functions, e.g. cylinders or spheres, then the complete solution for electric field due to the source charges located at far away positions and the induced charges on the surface of the object could be obtained by solving Laplace's equation considering the field region to be free from any volume charge. However, in order to get the complete solution appropriate boundary conditions on the surface of the object, whether it is conducting or dielectric, need to be satisfied. One of the common methods of getting the analytical solution for cylinder or sphere in uniform external field is the method of separation of variables as described in this chapter.

Sphere in Uniform External Field

Consider a spherical object of radius *a* within a uniform external field as shown in Fig.10.1. Since the boundary is a sphere of *r=constant,* hence the system is best described in spherical coordinates as shown in Fig.10.1. The uniform external field is given by $\vec{E}_0 = -E_0\hat{u}_z$ and the potential at any point due to the external field is given by $E_0 r\cos\theta = E_0 z$ with respect to the center of the sphere. In order to get the complete solution for electric field in this system, Laplace's equation in spherical coordinates as given in eqn.(10.1) needs to be solved.

$$\frac{1}{r^2}\frac{\partial}{\partial r}\left(r^2\frac{\partial V}{\partial r}\right)+\frac{1}{r^2\sin\theta}\frac{\partial}{\partial\theta}\left(\sin\theta\frac{\partial V}{\partial\theta}\right)+\frac{1}{r^2\sin^2\theta}\frac{\partial^2 V}{\partial\phi^2}=0 \qquad \text{…. 10.1}$$

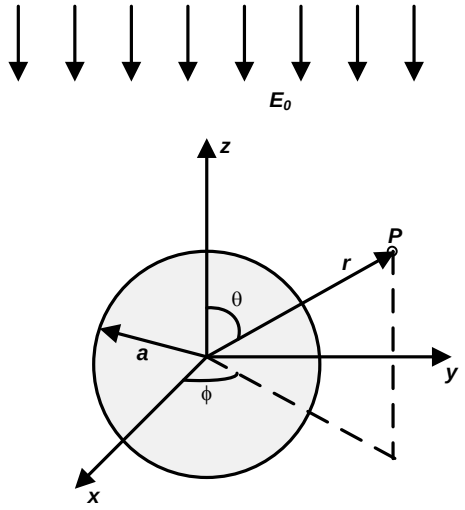

Fig.10.1 Sphere in uniform external field

The field system has azimuthal symmetry wrt the *z*-axis, i.e. the field system does not change with the rotation around the *z*-axis. So *z*-axis is made the polar axis in the spherical coordinate system. Then the field is independent of coordinate ϕ and the Laplace's equation reduces to

$$\frac{1}{r^2}\frac{\partial}{\partial r}\left(r^2\frac{\partial V}{\partial r}\right)+\frac{1}{r^2\sin\theta}\frac{\partial}{\partial\theta}\left(\sin\theta\frac{\partial V}{\partial\theta}\right)=0 \qquad \text{…. 10.2}$$

In order to separate the terms of the LHS of eqn.(10.2) into functions of only one variable, eqn.(10.2) may be rewritten by multiplying r^2 as

$$\frac{\partial}{\partial r}\left(r^2\frac{\partial V}{\partial r}\right)+\frac{1}{\sin\theta}\frac{\partial}{\partial\theta}\left(\sin\theta\frac{\partial V}{\partial\theta}\right)=0 \qquad \text{…. 10.3}$$

Then LHS of eqn.(10.3) is the sum of two terms which are functions of only one variable each, i.e. the first term is function of *r* only while the second term is function of θ only. The solution to eqn.(10.3) can be obtained as the product of two functions of which one is dependent only on *r* while the other is dependent only on θ.

Let the assumed solution be $V(r,\theta)=M(r)\,N(\theta)$ …. 10.4

The assumed solution is convenient as the boundary lies at *r=constant*.

Combining eqn.(10.3) and (10.4)

$$\frac{\partial}{\partial r}\left(r^2\frac{\partial M(r)\,N(\theta)}{\partial r}\right)+\frac{1}{\sin\theta}\frac{\partial}{\partial\theta}\left(\sin\theta\frac{\partial M(r)\,N(\theta)}{\partial\theta}\right)=0$$

$$\text{or, } N(\theta)\frac{\partial}{\partial r}\left(r^2\frac{\partial M(r)}{\partial r}\right)+M(r)\frac{1}{\sin\theta}\frac{\partial}{\partial\theta}\left(\sin\theta\frac{\partial N(\theta)}{\partial\theta}\right)=0$$

Dividing by $M(r)N(\theta)$,

$$\frac{1}{M(r)}\frac{d}{dr}\left(r^2\frac{d\,M(r)}{dr}\right)+\frac{1}{N(\theta)}\frac{1}{\sin\theta}\frac{d}{d\theta}\left(\sin\theta\frac{dN(\theta)}{d\theta}\right)=0 \qquad \text{…. 10.5}$$

The partial derivatives become total derivatives in eqn.(10.5) as each term is dependent on only one coordinate.

The sum of two terms of the LHS of eqn.(10.5) could be zero only when the two terms are separately equal to opposite and equal constant terms as given in eqn.(10.6).

Equal and opposite separation constant solution:

$$\frac{1}{M(r)}\frac{d}{dr}\left(r^2\frac{dM(r)}{dr}\right)=+p \text{ and } \frac{1}{N(\theta)}\frac{1}{\sin\theta}\frac{d}{d\theta}\left(\sin\theta\frac{dN(\theta)}{d\theta}\right)=-p \qquad \text{…. 10.6}$$

where, p is a positive constant.
Another solution is obtained when the separation constant is zero. Hence,
Zero separation constant solution:

$$\frac{1}{M(r)}\frac{d}{dr}\left(r^2\frac{dM(r)}{dr}\right)=0 \quad \text{and} \quad \frac{1}{N(\theta)}\frac{1}{\sin\theta}\frac{d}{d\theta}\left(\sin\theta\frac{dN(\theta)}{d\theta}\right)=0 \qquad \ldots. 10.7$$

Each of the above-mentioned two solutions is to be obtained separately.
Determination of the zero separation constant solution:
The first term of eqn.(10.7) is $\frac{1}{M(r)}\frac{d}{dr}\left(r^2\frac{dM(r)}{dr}\right)=0$, where $M(r)$ is non-zero. So

$$\frac{d}{dr}\left(r^2\frac{dM(r)}{dr}\right)=0, \text{ or, } r^2\frac{dM(r)}{dr}=C_0, \text{ or, } \frac{dM(r)}{dr}=\frac{C_0}{r^2}$$

Integrating and incorporating constants of integration

$$M(r)=\frac{C_{10}}{r}+C_{20} \qquad \ldots. 10.8$$

Next the second term of eqn.(10.7) is $\frac{1}{N(\theta)}\frac{1}{\sin\theta}\frac{d}{d\theta}\left(\sin\theta\frac{dN(\theta)}{d\theta}\right)=0$, where $N(\theta)$ is non-zero. So

$$\frac{1}{\sin\theta}\frac{d}{d\theta}\left(\sin\theta\frac{dN(\theta)}{d\theta}\right)=0, \text{ or, } \frac{d}{d\theta}\left(\sin\theta\frac{dN(\theta)}{d\theta}\right)=0, \text{ or, } \sin\theta\frac{dN(\theta)}{d\theta}=A_0$$

Integrating and incorporating constant of integration

$$N(\theta)=A_{10}\ln\left(\tan\frac{\theta}{2}\right)+A_{20} \qquad \ldots. 10.9$$

Eqn.(10.9) becomes undefined for $\theta=\pi$. But this is not feasible in the given system as potential must be a continuous function. So, A_{10} should be zero in eqn.(10.9). Therefore,

$$N(\theta)=A_{20} \qquad \ldots. 10.10$$

Then from eqns.(10.4), (10.8) and (10.10), the zero separation constant solution can be obtained as

$$V(r,\theta)=\frac{C_1}{r}+C_2 \qquad \ldots. 10.11$$

where, $C_1=A_{20}C_{10}$ and $C_2=A_{20}C_{20}$.
Determination of the equal and opposite separation constant solution:
The first term of eqn.(10.6) is $\frac{1}{M(r)}\frac{d}{dr}\left(r^2\frac{dM(r)}{dr}\right)=+p$,

$$\text{or, } \frac{d}{dr}\left(r^2\frac{dM(r)}{dr}\right)=+pM(r) \qquad \ldots. 10.12$$

Putting $M(r)=Cr^n$ in eqn.(10.12)

$$\frac{d}{dr}\left(r^2 Cnr^{n-1}\right)=+pCr^n, \text{ or, } Cn(n+1)r^n=pCr^n, \text{ or, } n^2+n-p=0$$

$$\text{Hence, } n=\frac{1}{2}\left(-1\pm\sqrt{1+4p}\right) \qquad \ldots. 10.13$$

The second term of eqn.(10.6) is $\frac{1}{N(\theta)}\frac{1}{\sin\theta}\frac{d}{d\theta}\left(\sin\theta\frac{dN(\theta)}{d\theta}\right)=-p$,

$$\text{or, } \frac{1}{\sin\theta}\frac{d}{d\theta}\left(\sin\theta\frac{dN(\theta)}{d\theta}\right)=-pN(\theta) \qquad \ldots. 10.14$$

Putting $N(\theta)=B\cos\theta$ in eqn.(10.14), $\frac{d}{d\theta}\left(-B\sin^2\theta\right)=-pB\cos\theta\sin\theta$, or, p = 2.

Hence, from eqn.(10.13) n = +1, -2.

Therefore, $M(r)=C'r+\frac{C''}{r^{-2}}$ and $N(\theta)=B\cos\theta$ …. 10.15

From eqns.(10.4) and (10.15),

$$V(r,\theta)=\left(C_3r+\frac{C_4}{r^2}\right)\cos\theta \quad \text{…. 10.16}$$

where, $C_3=C'B$ and $C_4=C''B$.

The complete solution for potential function is uniquely given as a linear combination of the two solutions given by eqns.(10.11) and (10.16).

$$V(r,\theta)=\frac{C_1}{r}+C_2+\left(C_3r+\frac{C_4}{r^2}\right)\cos\theta \quad \text{…. 10.17}$$

where, the constants are determined by satisfying the boundary conditions.

It is evident from eqn.(10.17) that the first term corresponds to a net charge on the sphere and the second term to a finite potential.

Conducting Sphere in Uniform Field

Consider that the sphere is a conducting one and is isolated and uncharged. Further, consider that the potential at the location of the center of the sphere due to the external field is V_0.

Since the perturbing action of the sphere is negligible at a large distance from the sphere, the potential at a large distance from the sphere ($r>>a$) is given by

$$V(r,\theta)=V_0+E_0r\cos\theta \quad \text{…. 10.18}$$

If the sphere is charged with a finite amount of charge Q, then

$$V(r,\theta)=\frac{Q}{4\pi\varepsilon_0 r}+V_0+E_0r\cos\theta \quad \text{…. 10.19}$$

In practical systems, floating metallic particles are usually not charged and hence eqn.(10.18) is taken here for further discussion.

Comparing eqns.(10.17) and (10.18) for r$\to\infty$, $C_2=V_0$, $C_3=E_0$. C_1 will be zero for uncharged sphere.

So, eqn.(10.17) can be rewritten as $V(r,\theta)=V_0+\left(E_0r+\frac{C_4}{r^2}\right)\cos\theta$ …. 10.20

On the conductor surface, i.e. for $r=a$, $V(a,\theta)=V_0+\left(E_0a+\frac{C_4}{a^2}\right)\cos\theta$ …. 10.21

But conducting sphere surface is an equipotential and hence electric potential is independent of θ on the conductor surface.

So, from eqn.(10.21), $C_4=-E_0a^3$

Hence, the complete solution for electric potential in the domain $r>a$ is given by

$$V(r,\theta)=V_0+E_0\left(r-\frac{a^3}{r^2}\right)\cos\theta \quad \text{…. 10.22}$$

The r and θ components of electric field intensity could be obtained as follows

$$E_r=-\frac{\partial V}{\partial r}=-E_0\left(1+\frac{2a^3}{r^3}\right)\cos\theta \quad \text{…. 10.23}$$

$$E_\theta = -\frac{1}{r}\frac{\partial V}{\partial \theta} = E_0\left(1-\frac{a^3}{r^3}\right)\sin\theta \quad \text{…. 10.24}$$

On the conducting sphere surface, tangential component of electric field intensity must be zero as it is an equipotential surface. Eqn.(10.24) shows that for $r=a$, E_θ is zero, which in turn validates the solution obtained.

Again, on the conducting sphere surface, E_r is the normal component of electric field intensity, which is given by $E_r\big|_{r=a} = -3E_0\cos\theta$. Thus the maximum value of electric field intensity on the surface of the conducting sphere is $3E_0$, i.e. three times the strength of uniform external field.

This is the reason why metallic dust particles should be avoided at all costs for gas insulated systems. Because presence of metallic dust particles will increase the local electric field intensity three times, which will result into partial discharge within the GIS that is very detrimental for GIS operation.

Induced surface charge density on the surface of the conducting sphere may be obtained as follows

$$\frac{\sigma_s}{\varepsilon_0} = E_r\Big|_{r=a} = -3E_0\cos\theta, \text{ or, } \sigma_s = -3\varepsilon_0 E_0\cos\theta \quad \text{…. 10.25}$$

As stated earlier, the sphere may be charged with an additional charge Q, which is distributed uniformly on the sphere surface and its effect on the field could be found by superposition.

Dielectric Sphere in Uniform Field

In the case of dielectric sphere present in a uniform external field, there will be two solutions to potential function, V_i valid for the region within the sphere having dielectric of permittivity ε_i and V_e valid for the region outside the sphere having dielectric of permittivity ε_e. So from eqn.(10.17)

$$V_i(r,\theta) = \frac{C_{1i}}{r} + C_{2i} + \left(C_{3i}r + \frac{C_{4i}}{r^2}\right)\cos\theta \quad \text{…. 10.26}$$

$$\text{and } V_e(r,\theta) = \frac{C_{1e}}{r} + C_{2e} + \left(C_{3e}r + \frac{C_{4e}}{r^2}\right)\cos\theta \quad \text{…. 10.27}$$

The potential at large distance r ($r>>a$) from the sphere

$$V(r,\theta) = V_0 + E_0 r\cos\theta \quad \text{…. 10.28}$$

where, V_0 is the potential at the location of the center of the sphere due to the external field.

Comparing eqns.(10.27) and (10.28) for $r\to\infty$, $C_{2e}=V_0$, $C_{3e}=E_0$. C_{1e} will be zero as a dielectric sphere is not considered to have any free charge.

Hence, eqn.(10.27) can be rewritten as $V_e(r,\theta) = V_0 + \left(E_0 r + \frac{C_{4e}}{r^2}\right)\cos\theta$ …. 10.29

Inside the dielectric sphere electric potential must be finite at all the points. Hence, from eqn.(10.26) $C_{1i}=C_{4i}=0$, $C_{2i}=V_0$. Hence, eqn.(10.26) can be rewritten as

$$V_i(r,\theta) = V_0 + C_{3i}r\cos\theta \quad \text{…. 10.30}$$

At $r=a$, both eqns.(10.29) and (10.30) should yield the same electric potential. Therefore,

$$V_0 + \left(E_0 a + \frac{C_{4e}}{a^2}\right)\cos\theta = V_0 + C_{3i}a\cos\theta$$

or, $E_0 a + \frac{C_{4e}}{a^2} = C_{3i}a$ …. 10.31

On the dielectric-dielectric boundary the normal component of electric field intensity should be same on both sides of the boundary. For the spherical boundary, *r*-component of electric field intensity is the normal component on the boundary. Hence,

$$-\varepsilon_i \left(\frac{\partial V_i}{\partial r}\right)\Bigg|_{r=a} = -\varepsilon_e \left(\frac{\partial V_e}{\partial r}\right)\Bigg|_{r=a}$$

or, $\varepsilon_i C_{3i} = \varepsilon_e \left(E_0 - \frac{2C_{4e}}{a^3}\right)$ …. 10.32

From eqns.(10.31) and (10.32)

$$C_{4e} = \frac{\varepsilon_e - \varepsilon_i}{2\varepsilon_e + \varepsilon_i} a^3 E_0$$

and $C_{3i} = \frac{3\varepsilon_e}{2\varepsilon_e + \varepsilon_i} E_0$

Therefore, the complete solutions for potential functions inside and outside the dielectric sphere are given by

$$V_i(r,\theta) = V_0 + \frac{3\varepsilon_e}{2\varepsilon_e + \varepsilon_i} E_0 r\cos\theta \quad \text{…. 10.33}$$

and $V_e(r,\theta) = V_0 + \left(r + \frac{\varepsilon_e - \varepsilon_i}{2\varepsilon_e + \varepsilon_i}\frac{a^3}{r^2}\right) E_0 \cos\theta$ …. 10.34

Noting that $r\cos\theta = z$, potential function inside the dielectric sphere can be written as

$$V_i(x,y,z) = V_0 + \frac{3\varepsilon_e}{2\varepsilon_e + \varepsilon_i} E_0 z \quad \text{…. 10.35}$$

Hence, electric potential within the dielectric sphere varies in only *z*-direction, i.e. the direction of the external field. Electric field intensity within the dielectric sphere will therefore have only the *z*-component, which is given by

$$E_{zi} = -\frac{\partial V_i}{\partial z} = -\frac{3\varepsilon_e}{2\varepsilon_e + \varepsilon_i} E_0 \quad \text{…. 10.36}$$

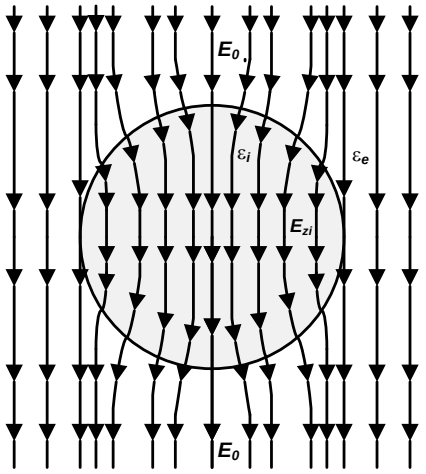

Fig.10.2 Electric field in and around dielectric sphere in uniform field

Eqn.(10.36) shows that the magnitude of electric field intensity within the dielectric sphere is constant. Typical field distribution in and around a dielectric sphere within a uniform external field is shown in Fig. 10.2.

Eqn.(10.36) also shows that if $\varepsilon_i < \varepsilon_e$, then $|E_{zi}| > E_0$. Consider the case of a spherical air bubble trapped within a moulded solid insulation of relative permittivity 4. If the magnitude of

electric field intensity in solid insulation at the location of the air bubble is E_0, then the magnitude of electric field intensity within the air bubble will be $1.33E_0$. The operating electric field intensity within solid insulation is usually kept at a higher value as the solid insulation has a higher dielectric strength and hence such increase in field intensity within the air bubble often causes partial discharge within the air bubble as the dielectric strength of air is much lower than solid insulation.

Cylinder in Uniform External Field

Consider a long cylindrical object of radius *a* within a uniform external field as shown in Fig.10.3. Since the boundary is a circle of *r=constant* on the *x-y* plane, hence the system is best described in cylindrical coordinates as shown in Fig.10.3. The uniform external field is given by $\vec{E}_0 = -E_0\hat{i}$ and the potential at any point due to the external field is given by $E_0 r\cos\theta = E_0 x$ with respect to the axis of the cylinder. In order to get the complete solution for electric field in this system, Laplace's equation in cylindrical coordinates as given in eqn.(10.37) needs to be solved.

$$\frac{1}{r}\frac{\partial}{\partial r}\left(r\frac{\partial V}{\partial r}\right)+\frac{1}{r^2}\frac{\partial^2 V}{\partial\theta^2}+\frac{\partial^2 V}{\partial z^2}=0 \qquad \text{…. 10.37}$$

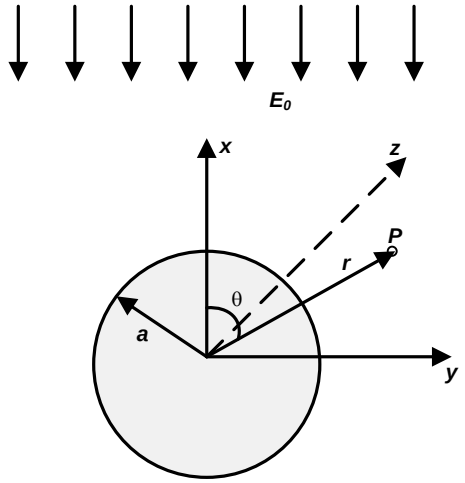

Fig.10.3 Cylinder in uniform external field

For this arrangement electric field distribution does not vary along the length of the cylinder, i.e. along *z*-coordinate. Hence, Laplace's equation reduces to

$$\frac{1}{r}\frac{\partial}{\partial r}\left(r\frac{\partial V}{\partial r}\right)+\frac{1}{r^2}\frac{\partial^2 V}{\partial\theta^2}=0 \qquad \text{…. 10.38}$$

Separating the terms of the LHS into functions of only one variable by multiplying r^2 with eqn.(10.38), it may be written that

$$r\frac{\partial}{\partial r}\left(r\frac{\partial V}{\partial r}\right)+\frac{\partial^2 V}{\partial\theta^2}=0 \qquad \text{…. 10.39}$$

The two terms on the LHS of eqn.(10.39) are functions of only one variable each, i.e. the first term is function of *r* only while the second term is function of θ only. The solution to eqn.(10.39) can be obtained as the product of two functions of which one is dependent only on *r* while the other is dependent only on θ.

Let the assumed solution be $V(r,\theta)=M(r)\,N(\theta)$ …. 10.40

The assumed solution is convenient as the boundary lies at *r=constant*.

Combining eqns.(10.39) and (10.40),

$$r\frac{\partial}{\partial r}\left(r\frac{\partial M(r)N(\theta)}{\partial r}\right)+\frac{\partial^2 M(r)N(\theta)}{\partial\theta^2}=0$$

or, $N(\theta)\left[r\frac{\partial}{\partial r}\left(r\frac{\partial M(r)}{\partial r}\right)\right]+M(r)\frac{\partial^2 M(r)N(\theta)}{\partial\theta^2}=0$

Dividing by $M(r)N(\theta)$,

$$\frac{r}{M(r)}\frac{d}{dr}\left(r\frac{dM(r)}{dr}\right)+\frac{1}{N(\theta)}\frac{d^2N(\theta)}{d\theta^2}=0 \qquad \text{…. 10.41}$$

The partial derivatives become total derivatives in eqn.(10.41) as each term is dependent on only one coordinate.

As in the case of sphere in uniform field, zero separation constant solution and equal and opposite separation constant solution are to be obtained separately in this case, too.

Determination of the zero separation constant solution:

The first term of eqn.(10.41) is $\frac{r}{M(r)}\frac{d}{dr}\left(r\frac{dM(r)}{dr}\right)=0$, where $M(r)$ is non-zero. So

$\frac{d}{dr}\left(r\frac{dM(r)}{dr}\right)=0$, or, $r\frac{dM(r)}{dr}=C_0$, or, $\frac{dM(r)}{dr}=\frac{C_0}{r}$

Integrating and incorporating constants of integration

$$M(r)=C_{10}\ln r+C_{20} \qquad \text{…. 10.42}$$

Next the second term of eqn.(10.41) is $\frac{1}{N(\theta)}\frac{d^2N(\theta)}{d\theta^2}=0$, where $N(\theta)$ is non-zero. So

$$N(\theta)=A_{10}\theta+A_{20} \qquad \text{…. 10.43}$$

But, from eqns.(10.42) and (10.43), it can be seen that there is discontinuity of potential at $r=0$ and $\theta=\infty$, which are not feasible in the given arrangement as potential must be a continuous function. Hence, $C_{10}=A_{10}=0$ in eqns.(10.42) and (10.43).

Therefore, $V(r,\theta)=C_{20}\,A_{20}=C_1$ …. 10.44

Determination of the equal and opposite separation constant solution:

The first term of eqn.(10.41) is $\frac{r}{M(r)}\frac{d}{dr}\left(r\frac{dM(r)}{dr}\right)=+p$, where p is a positive constant

or, $r^2\frac{d^2M(r)}{dr^2}+r\frac{dM(r)}{dr}=+pM(r)$ …. 10.45

Substituting $M(r)=Cr^n$ in eqn.(10.45), it may be obtained that

$n(n-1)+n=p$, or, $n=\pm\sqrt{p}$

Hence, $M(r)=\frac{C'}{r^{\sqrt{p}}}+C''r^{\sqrt{p}}$ …. 10.46

Again, the second term of eqn.(10.41) is $\frac{1}{N(\theta)}\frac{d^2N(\theta)}{d\theta^2}=-p$

or, $\frac{d^2N(\theta)}{d\theta^2}=-pN(\theta)$ …. 10.47

Substituting $N(\theta)=e^{a\theta}$ in eqn.(10.47), it may be obtained that

$a^2e^{a\theta}=-pe^{a\theta}$, or, $a=\pm i\sqrt{p}$

Hence, $N(\theta)=B\cos\left(\sqrt{p}\theta+\alpha\right)$ …. 10.48

Eqns.(10.46) and (10.48) lead to

$$V(r,\theta)=M(r)\,N(\theta)=\left(\frac{C_2}{r^{\sqrt{p}}}+C_3 r^{\sqrt{p}}\right)\cos\left(\sqrt{p}\theta+\alpha)\right) \quad \text{…. 10.49}$$

where, $C_2=C'B$ and $C_3=C''B$

From eqns.(10.44) and (10.49), the complete solution for potential function at all values of r and θ can be obtained as

$$V(r,\theta)=C_1+\left(\frac{C_2}{r^{\sqrt{p}}}+C_3 r^{\sqrt{p}}\right)\cos\left(\sqrt{p}\theta+\alpha)\right) \quad \text{…. 10.50}$$

The potential at large distance r ($r>>a$) from the cylinder is given by

$$V(r,\theta)=V_0+E_0\,r\cos\theta \quad \text{…. 10.51}$$

Matching eqns.(10.50) and (10.51), $\sqrt{p}=1$ and α=0.

Hence, the complete solution as given by eqn.(10.50) reduces to

$$V(r,\theta)=C_1+\left(\frac{C_2}{r}+C_3 r\right)\cos\theta \quad \text{…. 10.52}$$

Conducting Cylinder in Uniform Field

Comparing eqns.(10.51) and (10.52), $C_1=V_0$ and $C_3=E_0$.

So, $V(r,\theta)=V_0+\left(\frac{C_2}{r}+E_0 r\right)\cos\theta$

On the conductor surface, i.e. for $r=a$, $V(a,\theta)=V_0+\left(\frac{C_2}{a}+E_0 a\right)\cos\theta$ …. 10.53

But conducting cylinder surface is an equipotential and hence electric potential is independent of θ on the conductor surface.

So, from eqn.(10.53), $C_2=-E_0\,a^2$

Hence, the complete solution for electric potential in the domain $r>a$ is given by

$$V(r,\theta)=V_0+E_0\left(r-\frac{a^2}{r}\right)\cos\theta \quad \text{…. 10.54}$$

The r and θ components of electric field intensity could be obtained as follows

$$E_r=-\frac{\partial V}{\partial r}=-E_0\left(1+\frac{a^2}{r^2}\right)\cos\theta \quad \text{…. 10.55}$$

$$E_\theta=-\frac{1}{r}\frac{\partial V}{\partial \theta}=E_0\left(1-\frac{a^2}{r^2}\right)\sin\theta \quad \text{…. 10.56}$$

Eqn.(10.56) shows that for $r=a$, E_θ is zero, i.e. the tangential component of electric field intensity is zero on the cylindrical conductor surface as it is an equipotential surface.

Again, on the conducting cylinder surface, E_r is the normal component of electric field intensity, which is given by $E_r\big|_{r=a}=-2E_0\cos\theta$. Thus the maximum value of electric field intensity on the surface of the conducting cylinder is $2E_0$, i.e. twice the magnitude of uniform external field. Comparing this maximum electric field intensity with the value obtained for conducting sphere in uniform field, it may be seen that the enhancement of field intensity is more if the conducting object is spherical is shape.

Induced surface charge density on the surface of the conducting cylinder may be obtained as follows

$$\frac{\sigma_s}{\varepsilon_0} = E_r\Big|_{r=a} = -2E_0\cos\theta, \text{ or, } \sigma_s = -2\varepsilon_0 E_0\cos\theta \quad \text{…. 10.57}$$

Dielectric Cylinder in Uniform Field

Potential function valid for the region within the cylinder having dielectric of permittivity ε_I is

$$V_i(r,\theta) = C_{1i} + \left(\frac{C_{2i}}{r} + C_{3i}r\right)\cos\theta \quad \text{…. 10.58}$$

and the potential function valid for the region outside the cylinder having dielectric of permittivity ε_e is

$$V_e(r,\theta) = C_{1e} + \left(\frac{C_{2e}}{r} + C_{3e}r\right)\cos\theta \quad \text{…. 10.59}$$

The potential at large distance r ($r>>a$) from the cylinder

$$V(r,\theta) = V_0 + E_0 r\cos\theta \quad \text{…. 10.60}$$

where, V_0 is the potential at the location of the axis of the cylinder due to the external field. Comparing eqns.(10.59) and (10.60) for r$\to\infty$, $C_{1e} = V_0$, $C_{3e} = E_0$.

Hence, eqn.(10.59) can be rewritten as $V_e(r,\theta) = V_0 + \left(\frac{C_{2e}}{r} + E_0 r\right)\cos\theta$ …. 10.61

Inside the dielectric cylinder electric potential must be finite at all the points. Hence, from eqn.(10.58) $C_{1i} = V_0$, $C_{2i} = 0$. Hence, eqn.(10.58) can be rewritten as

$$V_i(r,\theta) = V_0 + C_{3i} r\cos\theta \quad \text{…. 10.62}$$

At any point on the dielectric cylinder surface, i.e. for $r=a$, electric potential as may be obtained from eqns.(10.61) and (10.62) must be unique. Hence,

$$\frac{C_{2e}}{a} + E_0 a = C_{3i}\, a \quad \text{…. 10.63}$$

From the boundary condition of normal component of electric flux density at $r=a$

$$-\varepsilon_i\left(\frac{\partial V_i}{\partial r}\right)\Big|_{r=a} = -\varepsilon_e\left(\frac{\partial V_e}{\partial r}\right)\Big|_{r=a}$$

or, $\varepsilon_i C_{3i} = \varepsilon_e\left(-\frac{C_{2e}}{a^2} + E_0\right)$ …. 10.64

From eqns.(10.63) and (10.64)

$$C_{2e} = \frac{\varepsilon_e - \varepsilon_i}{\varepsilon_e + \varepsilon_i} a^2 E_0$$

and $C_{3i} = \frac{2\varepsilon_e}{\varepsilon_e + \varepsilon_i} E_0$

Therefore, the complete solutions for potential functions inside and outside the dielectric cylinder are given by

$$V_i(r,\theta) = V_0 + \frac{2\varepsilon_e}{\varepsilon_e + \varepsilon_i} E_0 r\cos\theta \quad \text{…. 10.65}$$

and $V_e(r,\theta) = V_0 + \left(r + \frac{\varepsilon_e - \varepsilon_i}{\varepsilon_e + \varepsilon_i}\frac{a^2}{r}\right)E_0\cos\theta$ …. 10.66

As $r\cos\theta = x$, potential function inside the dielectric cylinder can be written as

$$V_i(x,y) = V_0 + \frac{2\varepsilon_e}{\varepsilon_e + \varepsilon_i} E_0\, x \qquad \text{…. 10.67}$$

Hence, electric potential within the dielectric cylinder varies in only *x*-direction, i.e. the direction of the external field. Electric field intensity within the dielectric cylinder will therefore have only the *x*-component, which is given by

$$E_{xi} = -\frac{\partial V_i}{\partial x} = -\frac{2\,\varepsilon_e}{\varepsilon_e + \varepsilon_i} E_0 \qquad \text{…. 10.68}$$

Similar to the case of dielectric sphere in uniform field, Eqn.(10.68) shows that the magnitude of electric field intensity within the dielectric cylinder is constant. Typical field distribution on the *x*-*y* plane in and around a dielectric cylinder within a uniform external field will be the same as that shown in Fig. 10.2.

As in the case of dielectric sphere in uniform field, for dielectric cylinder in uniform field also $|E_{zi}| > E_0$ if $\varepsilon_i < \varepsilon_e$. If a cylindrical air bubble is trapped within a moulded solid insulation of relative permittivity 4, then the magnitude of electric field intensity within the air bubble will be $1.6E_0$, where E_0 is the magnitude of electric field intensity in solid insulation at the location of the air bubble. Comparing this result with the corresponding value in the case of dielectric sphere, it may be seen that field enhancement is more if the gas cavity in liquid or solid insulation is cylindrical in shape.

Analytical Method

Field in cylinders, spheres, electrical cables etc, whose surfaces can be mathematically represented might be solved analytically.

- **Schwaigar's Utilisation Factor**

$$u = \frac{\text{Avg. Stress}}{\text{Max Stress}} = \frac{E_{av}}{E_{max}}$$

$$E_{av} = \frac{2V}{X}$$

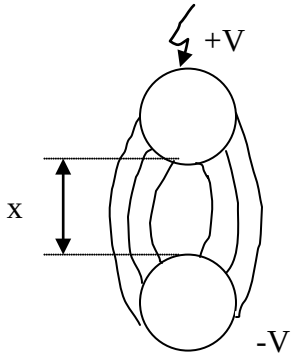

Average stress is defined as the potential difference between the electrodes divided by the distance. In most of the cases, maximum stress is on the electrode surface and is usually on the axis of symmetry, where the distance between the electrodes is minimum.

So, $u < 1$ -- In most of the practical cases

$u \approx 1$ – For uniform field

$u << 1 \longrightarrow$ For non-uniform field

u is a measure of non-uniformity of a field. If its value is very low, then the field is highly non-uniform. If u = 1, the field is uniform as in parallel plate arrangement.

Exception

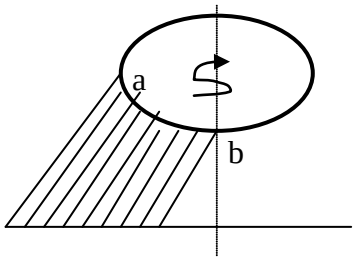

Though the pt. b is on the axis of symmetry and is at minimum distance from earth's surface, the maximum stress may take place at pt. a, for the arrangement shown.

When u is known, E_{max} can be easily determined as $E_{av} = V/X$ can be easily calculated

$$as \qquad E_{max} = \frac{E_{av}}{u}$$

In English literature, $f = \frac{1}{u} = \frac{E_{max}}{E_{av}}$

1. Concentric Sphere

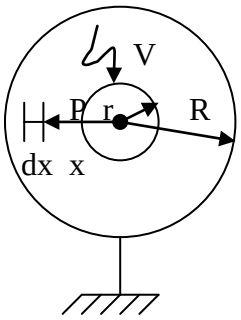

Let q be charge on the inner sphere.

The stress at $P = E = \frac{q}{4\pi\varepsilon x^2} = \frac{D}{\varepsilon}$

$$V = \int_r^R E dx = \frac{q}{4\pi\varepsilon}\int_r^R \frac{dx}{x^2}$$

$$= \frac{q}{4\pi\varepsilon}\left(\frac{1}{r} - \frac{1}{R}\right)$$

$$or, \quad \frac{q}{4\pi\varepsilon} = \frac{V}{\left(\frac{1}{r} - \frac{1}{R}\right)}$$

The maximum stress occurs on the surface of the inner sphere, where x = r

$$\text{So,} \quad E_{max} = \frac{q}{4\pi\varepsilon r^2} = \frac{V}{r^2\left(\frac{1}{r} - \frac{1}{R}\right)} = \frac{V}{r - \frac{r^2}{R}}$$

$$\text{and} \quad E_{av} = \frac{V}{R - r}$$

$$\text{Hence,} \quad u = \frac{E_{av}}{E_{max}} = \frac{V}{R - r} \cdot \frac{r\left(1 - \frac{r}{R}\right)}{V} = \frac{r}{R}$$

So, when r approaches R, the field will be more uniform.

Capacitance of the System

$$C = \frac{q}{V} = \frac{4\pi\varepsilon}{\frac{1}{r} - \frac{1}{R}} = \frac{4\pi\varepsilon_r\varepsilon_o}{\frac{1}{r} - \frac{1}{R}} = \frac{4\pi}{36\pi} \cdot \frac{\varepsilon_r \times 10^{-9}}{\frac{1}{r} - \frac{1}{R}}$$

$$C = \frac{\varepsilon_r}{9\left(\frac{1}{r} - \frac{1}{R}\right)} \times 10^{-9} F$$

2. Concentric Cylinders

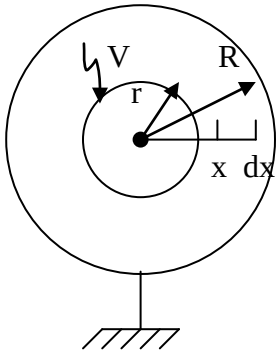

q - Charge on the inner cylinder per unit length

$$E = \frac{q}{2\pi\varepsilon x}$$

$$V = \int_r^R E dx = \frac{q}{2\pi\varepsilon} \int_r^R \frac{dx}{x}$$

$$= \frac{q}{2\pi\varepsilon} \ln\left(R/r\right)$$

or, $$\frac{q}{2\pi\varepsilon} = \frac{V}{\ln\left(R/r\right)}$$

Hence, $$E_{\max} = \frac{q}{2\pi\varepsilon r} = \frac{V}{r \ln\left(R/r\right)}$$

and $$E_{av} = \frac{V}{R - r}$$

So, $$u = \frac{E_{av}}{E_{\max}} = \frac{V}{R - r} \cdot \frac{r \ln \cdot R/r}{V} = \frac{\ln R/r}{\frac{R}{r} - 1}$$

Therefore, u is a function of (R/r).

So, if R/r ratio remains the same, u remains the same.

Capacitance of the system

$$C = \frac{q}{V} = \frac{2\pi\varepsilon}{\ln R/r} \; F/m \; \left[\text{capacitance per unit length}\right]$$

$$= \frac{2\pi\varepsilon_r \times 10^{-9}}{36\pi \ln R/r} \; F/m$$

$$= \frac{\varepsilon_r \times 10^{-9}}{18 \ln R/r} \; F/m = \frac{\varepsilon_r}{18 \ln R/r} \; \mu F / km$$

Method of Images

Image of a Point Charge wrt a Grounded Conducting Sphere

Image of a charge is not necessarily to be taken wrt infinitely long plane only. It can also be taken wrt curved surfaces like sphere, cylinder etc. To elaborate this issue, consider a point charge $+Q$ located at distance d from the center (O) of the sphere of radius a ($a<d$), as shown in Fig.9.4. Consider also that the electric potential of the sphere is zero. The field due to the point charge and the grounded sphere in the region outside the sphere could be determined by replacing the grounded sphere by an image charge. From the symmetry of the system it is evident that the image charge q will of negative polarity and will be located inside the sphere on the line joining the center of the sphere and the point charge, as shown in Fig.9.4. However, in this case the magnitude of q will not be equal to Q because such a pair of charges will not result into a zero potential spherical surface of radius a as required by the boundary condition.

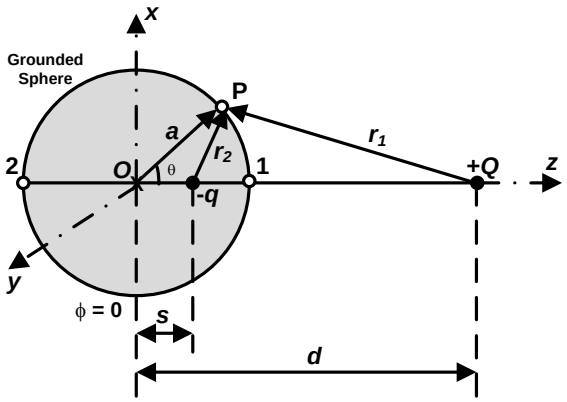

Fig.9.4 Point charge near a grounded sphere

Consider that the image charge is located at a distance s from the center of the sphere as shown in Fig.9.4. Now the problem is to determine the magnitude as well as the location of the image charge that satisfies the zero potential boundary condition for the spherical surface. With reference to Fig.9.4, the potential at the point P due to the point charge and its image is given by

$$\phi_P = \frac{1}{4\pi\varepsilon_0}\left(\frac{Q}{r_1} - \frac{q}{r_2}\right) \qquad \text{…. 9.9}$$

Imposition of the boundary condition $\phi_P = 0$ leads to

$$\frac{q}{Q} = \frac{r_2}{r_1} = \alpha \qquad \text{…. 9.10}$$

If α is kept constant, then $\frac{r_2}{r_1}$ =*constant* is the equation of a sphere. Hence, the problem now is to find the constant α.

For the point 1 as shown in Fig.9.4 $\alpha = \frac{r_2}{r_1} = \frac{a-s}{d-a}$

and for the point 2 as shown in Fig.9.4 $\alpha = \frac{r_2}{r_1} = \frac{a+s}{d+a}$

So, $\alpha = \frac{r_2}{r_1} = \frac{a-s}{d-a} = \frac{a+s}{d+a} = \frac{a}{d} = \frac{s}{a}$ (by componendo-dividendo) …. 9.11

Since, the radius of the sphere and the location of the point charge are known, hence the constant α can be computed from the ratio of *a* and *d*, as given by eqn.(9.11).

Therefore, the magnitude of the image charge is given by $q = \frac{a}{d}Q$ …. 9.12

and the location of the image charge is given by $s = \frac{a^2}{d}$ …. 9.13

Considering the line joining the point charge and its image passing through the center of the sphere to be along the *z*-axis and the center of the sphere to be the origin as shown in Fig.9.4, and also taking into account the spherical symmetry of the configuration, the field can be expressed in spherical coordinates as follows.

With reference to the point *P* of Fig.9.4,

$r_1 = \left|\vec{r}_P - \vec{r}_{+Q}\right| = \left(a^2 + d^2 - 2ad\cos\theta\right)^{1/2}$, where θ is the angle between *a* and *d* at the point *P*

$r_2 = \left|\vec{r}_P - \vec{r}_{-q}\right| = \left(a^2 + s^2 - 2as\cos\theta\right)^{1/2}$

Similarly, for any point in the field region for which *r* is the distance of the point from the origin, i.e. the center of the sphere, and θ is the angle between *r* and *d*

$r_1 = \left|\vec{r} - \vec{r}_{+Q}\right| = \left(r^2 + d^2 - 2rd\cos\theta\right)^{1/2}$ and

$$r_2 = \left|\vec{r} - \vec{r}_{-q}\right| = \left(r^2 + s^2 - 2rs\cos\theta\right)^{1/2} = \left(r^2 + \frac{a^4}{d^2} - 2r\frac{a^2}{d}\cos\theta\right)^{1/2} = \left(\frac{r^2d^2 + a^4 - 2rda^2\cos\theta}{d^2}\right)^{1/2}$$

So, electric potential at any point due to the point charge and its image is given by

$$\phi(r,\theta) = \frac{Q}{4\pi\varepsilon_0}\left[\frac{1}{\left(r^2 + d^2 - 2rd\cos\theta\right)^{1/2}} - \frac{a}{\left(r^2d^2 + a^4 - 2rda^2\cos\theta\right)^{1/2}}\right] \quad \text{…. 9.14}$$

So, $\vec{E}_r(a,\theta) = -\left.\frac{\partial\phi(r,\theta)}{\partial r}\right|_{r=a} = -\frac{Q}{4\pi\varepsilon_0 a}\frac{d^2 - a^2}{\left(a^2 + d^2 - 2ad\cos\theta\right)^{3/2}}$ …. 9.15

Now, *r*-component of electric field intensity is the normal component on the sphere surface. So, assuming the induced surface charge density on the sphere surface to be σ_s, the normal component of electric field intensity is equal to $\frac{\sigma_s}{\varepsilon_0}$ just off the sphere surface. Equating this expression with the one given by eqn.(9.15), the induced surface charge density on the grounded sphere surface is given by

$$\sigma_s = -\frac{Q}{4\pi a}\frac{d^2 - a^2}{\left(a^2 + d^2 - 2ad\cos\theta\right)^{3/2}} \quad \text{…. 9.16}$$

Method of Successive Images

Sphere gap arrangements are very commonly used in high voltage system for voltage measurement. As shown in Fig.9.5, in this arrangement two spheres of identical radii are separated by a specific distance *s*, where one sphere is charged while the other is earthed. The field within the sphere gap due to the two spheres could be analyzed with the help of image charges as described in section 9.3. The live sphere of potential *V* is at first replaced by a charge of magnitude $Q_A = 4\pi\varepsilon_0 aV$ located at the center of the live sphere. Then to keep the potential of the grounded sphere at zero, $-q_1$ is introduced within the grounded sphere which is the image of Q_A, as shown in Fig.9.5. The magnitude and location of q_1 are given by

$$q_1 = \frac{a}{d} Q_A \qquad \text{and} \qquad s_1 = \frac{a^2}{d} \qquad \ldots. 9.17$$

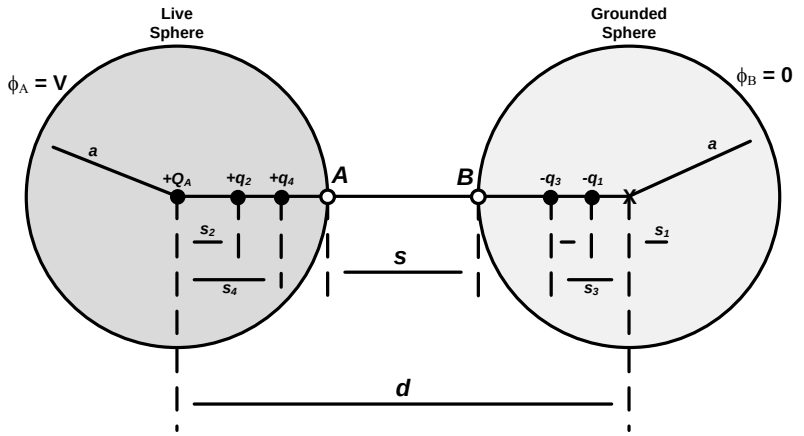

Fig.9.5 Method of successive imaging as applied to sphere gap arrangement

But the introduction of $-q_1$ will make the potential of live sphere different from V. So to keep the potential of live sphere equal to V, $+q_2$, which is the image of $-q_1$, is introduced within the live sphere such that the potential of live sphere due to $+q_2$ and $-q_1$ will be zero. As a result, the potential of live sphere due to $+Q_A$, $-q_1$ and $+q_2$ will be again V. The magnitude and location of q_2 are given by

$$q_2 = \frac{a}{d - s_1} q_1 = \frac{a^2}{d(d - s_1)} Q_A \quad \text{and} \quad s_1 = \frac{a^2}{d - s_1} \qquad \ldots. 9.18$$

But the introduction of $+q_2$ will make the potential of grounded sphere different from zero. So $-q_3$ is introduced within the grounded sphere as the image of $+q_2$ to make the potential of the grounded sphere equal to zero. Further, introduction of $-q_3$ warrants introduction of $+q_4$ within the live sphere and so on. In this way there will be an infinite series of charges within the two spheres: positive charges such as $+Q_A$, $+q_2$, $+q_4$ within the live sphere and negative charges such as $-q_1$, $-q_3$ within the grounded sphere. This method of taking successive image charges within the two spheres is known as method successive imaging. It may be seen from eqns.(9.17) and (9.18) that each successive image charge is smaller in magnitude and gradually shifts towards the surface of the sphere within which it is located. In all practicality it is adequate to take the first few images within the two spheres to achieve reasonably good accuracy in the computation of electric field. In the sphere gap arrangement, maximum value of electric field intensity occurs at the so called sparking tips of the spheres, viz. points A and B as shown in Fig.9.5. This maximum electric field intensity can be obtained as

$$E_{\max} = \frac{V}{s} \left[\frac{\frac{s}{a} + 1 + \sqrt{\left(\frac{s}{a} + 1\right)^2 + 8}}{4} \right] \qquad \ldots. 9.19$$

As discussed in section 4.7, $E_{av} = \dfrac{V}{s}$

So, field factor (f) for sphere gap arrangement = $\dfrac{E_{\max}}{E_{av}} = \left[\dfrac{\frac{s}{a} + 1 + \sqrt{\left(\frac{s}{a} + 1\right)^2 + 8}}{4} \right]$ $\ldots. 9.20$

Variation of field factor (f) with gap distance (s) in the case of sphere gap arrangement is presented in Table 9.1. It may be seen from Table 9.1 that the deviation from uniform field (f=1) for s/a=0.2 is 6.8% while that for s/a=1.0 is 36.6%. Accuracy of voltage measurement by sphere gap depends significantly on the degree of field non-uniformity between the two spheres. Hence, it is recommended in practice that the gap distance should not be made more than the radius of the spheres.

Table 9.1
Variation of field factor with gap distance for sphere gap

s/a	0.2	0.4	0.6	0.8	1.0
f	1.068	1.139	1.212	1.288	1.366

Problem 9.1
Two spheres of 25cm diameter have a gap distance of 2.5cm between them. Determine the breakdown voltage of the sphere gap in air at STP.
Solution
Given, s = 2.5cm and a = (25/2) = 12.5cm

So, $\frac{s}{a}=\frac{2.5}{12.5}=0.2$ Correspondingly, field factor (f) = 1.068

E_{max} corresponding to breakdown of air at STP is 30kV$_p$/cm.

So, $E_{av}=\frac{E_{\max}}{f}=\frac{30}{1.068}=28.09\,\text{kV}_\text{p}/\text{cm}$

But, $E_{av}=\frac{V}{s}$ Hence, $\frac{V}{2.5}=28.09$, or, V = 70.22 kV$_p$.

Two Infinitely Long Parallel Cylinders

Electric field due to two parallel cylindrical transmission line conductors is the same as the field due to two infinitely long parallel cylinders. The cross-sectional view of the arrangement is shown in Fig.9.9. Electric field for this arrangement is two-dimensional in Cartesian coordinates, because the field does not vary along the z-axis, which is along the length of the cylinders. Electric field varies only on the cross-sectional plane which is taken as the x-y plane. As discussed in section 9.4, these two parallel cylinders having potential $+V$ and $-V$ could be replaced by two infinitely long line charges of uniform line charge density $+\lambda_l$ and $-\lambda_l$ located within the respective cylinders as shown in Fig.9.9. These two line charges together will create two cylindrical equipotential surfaces of radius a having the prescribed potentials $+V$ and $-V$. The charges will be located at a distance s from the axis of the respective cylinders. So the problem is to find the location of these charges.

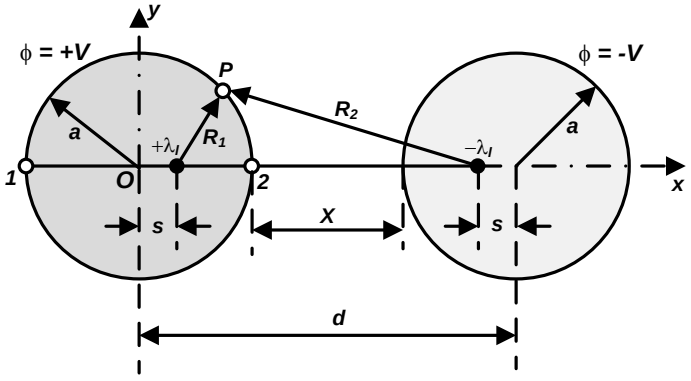

Fig.9.9 Two infinitely long parallel cylinders replaced by two infinitely long line charges

With reference to Fig.9.9, the potential of the point *P* on the surface of the cylinder is

$$\phi_P = \frac{\lambda_l}{2\pi\varepsilon_0}\ln\frac{R_2}{R_1}$$

For the cylinder surface to be equipotential the ratio of R_2 to R_1 must be constant.
Considering the point *1* on the cylinder surface as shown in Fig.9.9,

$$\phi_1 = \frac{\lambda_l}{2\pi\varepsilon_0}\ln\frac{d+a-s}{a+s} \qquad \text{…. 9.29}$$

and for the point *2* on the cylinder surface as shown in Fig.9.9,

$$\phi_2 = \frac{\lambda_l}{2\pi\varepsilon_0}\ln\frac{d-a-s}{a-s} \qquad \text{…. 9.30}$$

But, $\phi_1=\phi_2$. Hence, $\frac{d+a-s}{a+s}=\frac{d-a-s}{a-s}=\frac{d-s}{a}=\frac{a}{s}$ (by componendo-dividendo)

Therefore, $s^2 - sd + a^2 = 0$

or, $s = \frac{d}{2} \pm \frac{\sqrt{d^2-4a^2}}{2}$ …. 9.31

In the solution of *s* as given by eqn.(9.31), the additive expression has to be neglected, because in that case the image charge will be located outside the cylinder. Therefore,

$$s = \frac{d}{2} - \frac{\sqrt{d^2-4a^2}}{2} \qquad \text{…. 9.32}$$

For transmission lines, $d>>a$ and hence $s\approx 0$, i.e. the line charges are placed on the axes of the two cylinders.
Now, the potential at the point *2* on the cylinder surface, as shown in Fig.9.9, is $+V$. Hence,

$$\phi_2 = \frac{\lambda_l}{2\pi\varepsilon_0}\ln\frac{d-a-s}{a-s} = V$$

or, $\lambda_l = \frac{2\pi\varepsilon_0 V}{\ln\frac{d-a-s}{a-s}}$ …. 9.33

Eqn.(9.33) gives the magnitude of the uniform line charge density.
In the arrangement shown in Fig.9.9, maximum electric field intensity (E_{max}) occurs at the point *2*, which is given by

$$E_{\max} = \frac{\lambda_l}{2\pi\varepsilon_0}\left(\frac{1}{a-s}+\frac{1}{d-a-s}\right) = \frac{V}{\ln\frac{d-a-s}{a-s}}\left(\frac{1}{a-s}+\frac{1}{d-a-s}\right) \qquad \text{…. 9.34}$$

RHS of eqn.(9.34) is in terms of the physical dimensions of the arrangement and the electric potential of the cylinders and hence can be computed in a straightforward manner.

Again, for the physical arrangement of Fig.9.9, $E_{av} = \frac{2V}{d-2a}$

Therefore, field factor (*f*) = $\frac{E_{\max}}{E_{av}} = \frac{(d-2a)}{2\ln\frac{d-a-s}{a-s}}\left(\frac{1}{a-s}+\frac{1}{d-a-s}\right)$ …. 9.35

Putting the value of *s* from eqn.(9.32) in eqn.(9.35) and upon simplification it may be written that

$$f = \frac{\sqrt{\left(\frac{d}{2a}\right)^2 - 1}}{\ln\left[\frac{d}{2a} + \sqrt{\left(\frac{d}{2a}\right)^2 - 1}\right]} \quad \text{…. 9.36}$$

For transmission lines, eqn.(9.36) is often modified by putting $d=X+2a$, which yields

$$f = \frac{\sqrt{\left(\frac{X}{a}\right)^2 + 4\frac{X}{a}}}{2\ln\left[\frac{X}{2a} + 1 + \frac{1}{2}\sqrt{\left(\frac{X}{a}\right)^2 + 4\frac{X}{a}}\right]} \quad \text{…. 9.37}$$

Eqn.(9.37) represents the field factor as a function of the ratio of the gap distance between the two transmission line conductors (X) and the radius of the conductors (a).

For high voltage transmission lines, $d>>a$. As a result the field factor as given by eqn.(9.36) reduces to

$$f = \frac{d}{2a\ \ln\frac{d}{a}} \quad \text{…. 9.38}$$

and $E_{av} = \frac{2V}{d-2a} \approx \frac{2V}{d}$

Hence, $E_{\max} = E_{av} \times f = \frac{2V}{d} \times \frac{d}{2a\ln\frac{d}{a}} = \frac{V}{a\ln\frac{d}{a}}$ …. 9.39

Capacitance per unit length between the two parallel cylinders can be obtained from eqn.(9.32) and (9.33) as follows

$$C = \frac{\lambda_l}{2V} = \frac{\pi\varepsilon_0}{\ln\frac{d-a-s}{a-s}} = \frac{\pi\varepsilon_0}{\ln\left[\frac{d}{2a} + \sqrt{\left(\frac{d}{2a}\right)^2 - 1}\right]} \quad \text{…. 9.40}$$

Since, $\ln\left(x + \sqrt{x^2-1}\right) = \cosh^{-1} x$, hence for $x>1$ eqn.(9.40) can be written as

$$C = \frac{\pi\varepsilon_0}{\cosh^{-1}\left(\frac{d}{2a}\right)} \quad \text{…. 9.41}$$

Problem 9.2

A long conductor of negligible radius is at a height 5m from earth surface and is parallel to it. It has a uniform line charge density of +1nC/m. Find the electric potential and field intensity at a point 3m below the line.

Solution

The arrangement of the problem is shown in Fig.9.10. Since the conductor is considered to have negligible radius, hence the line charge is located on the axis of the conductor.

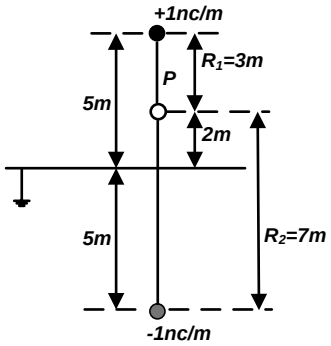

Fig.9.10 Pertaining to Problem 9.2

With reference to eqn.(9.25), λ_l=1nc/m, R_1=3m and R_2=7m.

So, $\phi_P = \frac{10^{-9}}{2\pi \times 8.854 \times 10^{-12}} \ln \frac{7}{3} = 15.23\, V$

Electric field intensity components at the point *P* are obtained from eqn.(9.26) as follows:

$E_{xP} = 0$

$$E_{yP} = \frac{10^{-9}}{2\pi \times 8.854 \times 10^{-12}} \left(\frac{2-5}{3^2} - \frac{2+5}{7^2} \right) = -8.56\, V/m$$

Problem 9.3

Determine the breakdown voltage in air at STP of a 20cm diameter cylindrical electrode placed horizontally with its axis 20cm above earth surface.

Solution

The arrangement of the problem is shown in Fig.9.11.

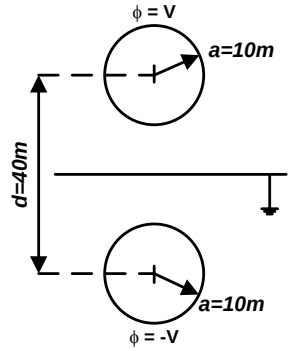

Fig.9.11 Pertaining to Problem 9.3

With reference to eqn.(9.36)

d = 40cm and *a* = 10cm. Hence, (*d*/*2a*) = 2

So, $f = \frac{\sqrt{2^2 - 1}}{\ln(2 + \sqrt{2^2 - 1})} = 1.315$

E_{max} corresponding to breakdown of air at STP is 30kV$_p$/cm.

So, $E_{av} = \frac{E_{\max}}{f} = \frac{30}{1.315} = 22.81\,\text{kV}_p/\text{cm}$

But, $E_{av} = \frac{2V}{d - 2a}$ Hence, $\frac{2V}{20} = 22.81$, or, V = 228.1 kV$_p$.

Conformal Mapping

Introduction

Analytical solutions to many field problems, particularly Dirichlet problems, can be obtained using methods like Fourier Series and integral transforms. These methods are applicable only for simple regions and the solutions are either infinite series or improper integrals, which are difficult to evaluate. Closed form solutions to many Dirichlet problems can be obtained using conformal mapping, which is a similarity transformation. If a function is harmonic, i.e. it satisfies Laplace's equation $\vec{\nabla}^2 f = 0$, then the transformation of such a function via conformal mapping is also harmonic. Hence, equations in relation to any field that can be represented by a potential function can be solved with the help of conformal mapping. However, conformal mapping can only be employed in two dimensional fields. If the solution for potential field is required in three dimensional cases, then conformal mapping is applicable to only those configurations where the potential field is translationally invariant along any one of the three axes. The two dimensional potential fields that can be solved by conformal mapping are static electric fields, static magnetic fields, static electric flow fields, stationary thermal flow fields, stationary hydrodynamic flow fields to name a few. According to Riemann Mapping Theorem any two regions with same connectivity may be conformally mapped to one another. But in practical applications conformal mapping is used only in those cases where the maps take simpler, explicit forms, so that one may carry out actual calculations with those maps.

As the application of conformal mapping is limited to variables which solve the Laplace's equation for two dimensional fields, one such variable of practical interest is the electrostatic potential in a region of space that is free of charges. This chapter, therefore, focuses on application of conformal mapping to determine electrostatic potential field by solving two dimensional Laplace's equation.

Basic Theory of Conformal Mapping

Conformal transformation is based on the properties of analytic functions. Let, $z = x + iy$ be a complex variable such that the real and imaginary parts x and y are real valued variables, and $f(z) = u(z) + iv(z) = u(x, y) + iv(x, y)$ be a complex valued function such that the real and imaginary parts u and v are real and single valued functions of real valued variables x and y.

If the derivative of *f(z)* exists at a point *z*, then the partial derivatives of u and v exist at that point and obey the Cauchy-Riemann equations as follows.

$$\frac{\partial u}{\partial x} = \frac{\partial v}{\partial y} \text{ and } \frac{\partial u}{\partial y} = -\frac{\partial v}{\partial x} \quad \text{…. 11.1}$$

A function *f(z)* is analytic at a point z_0 if its derivative $f'(z)$ exists not only at z_0 but at every point in the neighborhood of z_0. It can also be shown that if *f(z)* is analytic, the partial derivatives of u and v of all orders exist and are continuous functions of x and y. So,

$$\frac{\partial^2 u}{\partial x^2} = \frac{\partial}{\partial x}\left(\frac{\partial u}{\partial x}\right) = \frac{\partial}{\partial x}\left(\frac{\partial v}{\partial y}\right) = \frac{\partial^2 v}{\partial x \partial y} = \frac{\partial}{\partial y}\left(\frac{\partial v}{\partial x}\right) = \frac{\partial}{\partial y}\left(-\frac{\partial u}{\partial y}\right) = -\frac{\partial^2 u}{\partial^2 y}$$

or, $$\frac{\partial^2 u}{\partial x^2} + \frac{\partial^2 u}{\partial y^2} = 0 \quad \text{…. 11.2}$$

In the same way one may get, $\frac{\partial^2 v}{\partial x^2}+\frac{\partial^2 v}{\partial y^2}=0$ …. 11.3

Eqns.(11.2) and (11.3) show that both the functions *u(x,y)* and *v(x,y)* satisfy Laplace's equation.

Any function that has continuous second order partial derivatives and satisfies Laplace's equation is called a Harmonic function. Thus both the real part, *u(x,y)*, and imaginary part, *v(x,y)*, of the complex function *f(z)* are harmonic functions. If the function *f(z) = u(x,y)+iv(x,y)* is analytic, then *u(x,y)* and *v(x,y)* are conjugate harmonic functions. If one of two harmonic functions is known, then the other can be found using Cauchy-Riemann equations.

Thus both the conjugate harmonic functions *u(x,y)* and *v(x,y)* can be used to find the potential since they satisfy Laplace's equation.

Mapping of Shapes

From a different point of view, the complex function *f(z)* can be considered as a tool for change of variables, i.e. a transformation from the complex *z*-plane to the complex *w*-plane, as shown in Fig.11.1, where

$z=x+iy$ and $w=u+iv$

It can also be shown that if the function *f* is analytic at a point $z=z_0$ on the *z*-plane, where the first order derivative $f'(z_0)$ is non-zero, there exists a neighborhood of the point w_0 in the *w*-plane in which the function *w=f(z)* has a unique inverse *z=F(w)*. The functions *f(z)* and *F(w)*, therefore, define a change of variables from (*x,y*) to (*u,v*) and from (*u,v*) to (*x,y*), respectively.

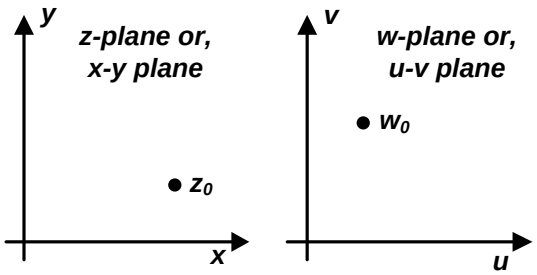

Fig.11.1 Mapping between *z*-plane and *w*-plane

On the *z*-plane, $dz=dx+i\,dy$ and on the *w*-plane $dw=du+i\,dv$

So, $|dz|^2=dx^2+dy^2$ …. 11.4

and $|dw|^2=du^2+dv^2$ …. 11.5

Then, on the *z*-plane, square of the length element can be written as

$dl^2=dx^2+dy^2=|dz|^2$ …. 11.6

and, on the *w*-plane, square of the length element can be written as

$dL^2=du^2+dv^2=|dw|^2$ …. 11.7

Therefore, from eqns.(11.6) and (11.7), it may be written that

$\frac{dL}{dl}=\left|\frac{dw}{dz}\right|$ …. 11.8

Thus, in the neighborhood of each point in *z*-plane, if *w(z)* is analytic and have a non-zero derivative, i.e. finite slope at that point, then the ratio of length elements in two planes remains constant. The net result of this transformation is to change the dimensions in equal

proportions and rotate each infinitesimal area in the neighborhood of that point. In general, a linear transformation $w = f(z) = a\,z + b$, where a and b are complex numbers, rotates by $arg(a)$ in the anti-clockwise direction, dilates or compresses by $|a|$ and translates by b. Thus the ratio of linear dimensions, which may also be represented as the angle, is preserved. As a result, conformal mapping is isogonic because it preserves angles. Hence, all curves in the z-plane that intersect each other at particular angles are mapped into curves in the w-plane that intersect each other at exactly the same angles. This property is most useful for electric field analysis as the equipotentials and the field lines, which are normal to each other in z-plane, are mapped to corresponding curves in w-plane, which are also mutually orthogonal.

Furthermore, $f'(z)F'(w) = \left|\frac{dw}{dz}\right|\left|\frac{dz}{dw}\right| = 1$, which means that the inverse mapping is also conformal. Because of this uniqueness and conformal property of inverse mapping, solution obtained in the w-plane can be mapped back to z-plane.

When infinitesimally small region is considered, then every shape in the z-plane is transformed into a similar shape in the w-plane, e.g. a rectangle in the z-plane remains a rectangle in w-plane. However, shape will not be preserved in general, particularly in a large scale as the value of $\left|\frac{dw}{dz}\right|$ may vary considerably at different points in the z-plane. As a result rotation and scaling will vary from one point in the z-plane to its neighboring point and hence the similarity of shape is not achieved for large regions.

At this juncture, it is pertinent to mention that conformal mapping does not provide a solution to any arbitrary problem. Another question that arises is why one should use conformal mapping instead of numerical methods. The answer to this question is two-fold: firstly analytical solutions to field problems provides insight and secondly it provides useful approximations to difficult problems, which in many cases is valuable to practicing engineers.

Preservation of Angles in Conformal Mapping

As shown in Fig.11.2, two curves A and B intersect each other at an angle α at the point z_i in the z-plane. With the help of the tangent vectors to the curves, the angle between the curves could be computed. Let, t_{zA} and t_{zB} be the tangent vectors to the curves A and B, respectively. Then from the law of cosines it may be written that

$$\alpha = \cos^{-1}\left(\frac{|t_{zA}|^2 + |t_{zB}|^2 - |t_{zA} - t_{zB}|^2}{2|t_{zA}||t_{zB}|}\right) \quad \text{…. 11.9}$$

The corresponding transformed curves A' and B' intersect at an angle β in the w-plane. Let, t'_{wA} and t'_{wB} be the tangent vectors to the curves A' and B', respectively. Then β can be obtained as

$$\beta = \cos^{-1}\left(\frac{|t'_{wA}|^2 + |t'_{wB}|^2 - |t'_{wA} - t'_{wB}|^2}{2|t'_{wA}||t'_{wB}|}\right) \quad \text{…. 11.10}$$

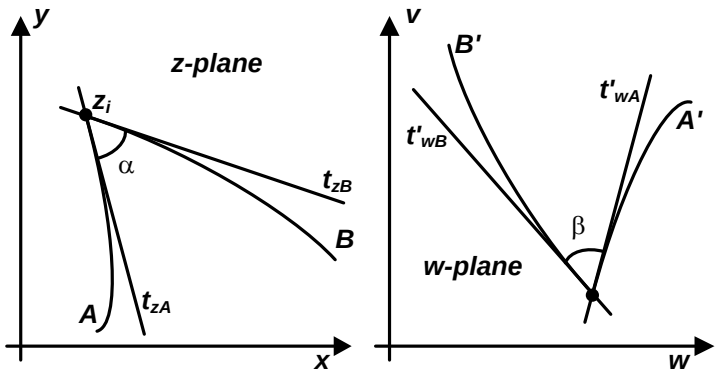

Fig.11.2 Preservation of angles in conformal mapping

Let, a curve is parameterized in *z*-plane by *z=z(p)* and the complex analytic function *w=f(z(p))* defines the mapped curve in the *w*-plane. Then application of chain rule to *w=f(z(p))* gives $t'_w = f'(z(p))t_z(p)$. Since the curves intersect in *z*-plane at $z=z_i$, then $t'_{wA} = f'(z_i)t_{zA}$ and $t'_{wB} = f'(z_i)t_{zB}$. Since $f'(z_i)\neq 0$, hence eqn.(11.10) can be re-written as

$$\beta = \cos^{-1}\left(\frac{\left|f'(z_i)t_{zA}\right|^2 + \left|f'(z_i)t_{zB}\right|^2 - \left|f'(z_i)t_{zA} - f'(z_i)t_{zB}\right|^2}{2\left|f'(z_i)t_{zA}\right|\left|f'(z_i)t_{zB}\right|}\right) \quad \text{…. 11.11}$$

In eqn.(11.11), the absolute value $\left|f'(z_i)\right|^2$ cancels from the numerator and denominator and eqn.(11.11) gets reduced to

$$\beta = \cos^{-1}\left(\frac{\left|t_{zA}\right|^2 + \left|t_{zB}\right|^2 - \left|t_{zA} - t_{zB}\right|^2}{2\left|t_{zA}\right|\left|t_{zB}\right|}\right) \quad \text{…. 11.12}$$

From eqns.(11.9) and (11.10), $\alpha = \beta$, which proves that angles are preserved in conformal mapping.

Problem 11.1

For the point *z=1+i* in the *z*-plane, find the mapped point in the *w*-plane under the linear transformation *w=(1+i)z +(2 +2i).*

Solution

The given transformation function $w = f(z) = (1+i)z + (2+2i) = \sqrt{2}e^{i\frac{\pi}{4}}z + (2+2i)$

Hence, the transformation of the point (*1+i*) in the *z*-plane to the corresponding point in the *w*-plane can be obtained in three steps as shown in Fig.11.3.

Step-1: The length *OP* $\left(\left|z\right|\right)$ is multiplied by $\left|1+i\right| = \sqrt{2}$ to get the length *AB* as shown in Fig.11.3(b).

Step-2: The length *AB* is rotated by an angle ($\pi/4$) in the anti-clockwise direction to get the length *AC*, as shown in Fig.11.3(c).

Step-3: The point *C* is then translated by (*2+2i*) to get the point *P′* (*2+4i*) in the *w*-plane which is the conformally mapped point corresponding to the point *P* in the *z*-plane.

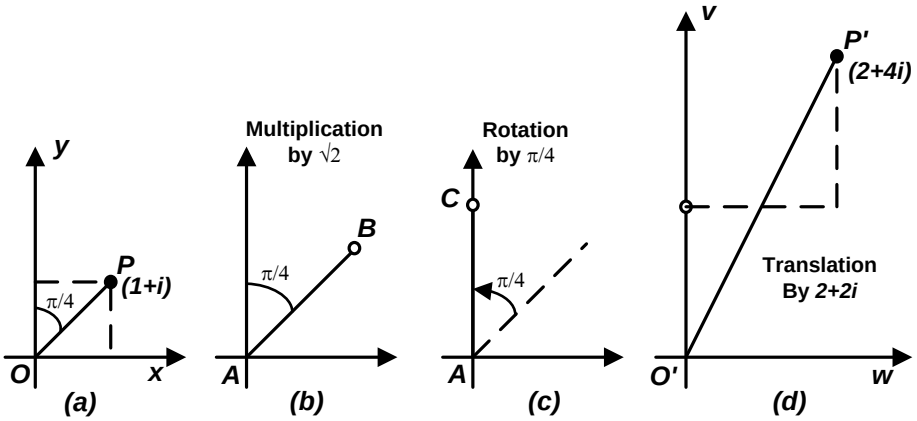

Fig.11.3 Pertaining to Problem 11.1

Problem 11.2

Let Ω be the rectangular region in the *z*-plane bounded by *x=1*, *y=1*, *x=3* and *y=2*. Find the mapped region Ω' in the *w*-plane under the linear transformation *w=(1+i)z +(2 +2i)*.

Solution

Given, $w=f(z)=(1+i)z + (2+2i) = (1+i)(x+iy) + (2+2i) = (x-y+2) + i\,(x+y+2)$

Hence, $u = x-y+2$ and $v = x+y+2$

Therefore, for $x=1$, $u = -y+3$ and $v = y+3$ or, $u+v = 6$, i.e. the line $x=1$ in the *z*-plane is mapped to the straight line $u+v=6$ in the *w*-plane.

Similarly, for $y=1$, $u = x+1$ and $v = x+3$ or, $u-v = -2$

For $x=3$, $u = -y+5$ and $v = y+5$ or, $u+v = 10$

For $y=2$, $u = x$ and $v = x+4$ or, $u-v = -4$

So, the four straight lines in the *z*-plane defined by *x=1*, *y=1*, *x=3* and *y=2* are mapped to four straight lines defined by $u+v = 6$, $u-v = -2$, $u+v = 10$ and $u-v = -4$, respectively, in the *w*-plane. The mapping is shown in Fig.11.4. Under the linear transformation $w=az+b$, where $a=1+i$ and $b=2+2i$, it may be seen that the rectangular region Ω in the *z*-plane is translated by $b(=2+2i)$, rotated by an angle 45^0 $(=arg(a)=arg(1+i))$ in the anti-clockwise direction and dilated by $\sqrt{2}(=|a|=|1+i|)$ to another rectangular region Ω' in the *w*-plane.

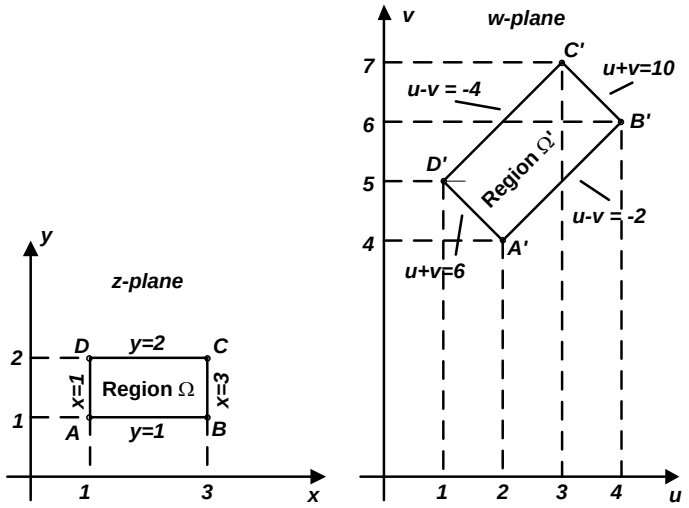

Fig.11.4 Pertaining to Problem 11.2

Concept of Complex Potential

Let, $\phi(x, y)$ be a harmonic function in a domain Ω. It is possible to define a harmonic conjugate function, $\psi(x, y)$, uniquely by Cauchy-Riemann equations in the same domain. Thus an analytic function of $z = x + iy$ in the domain Ω can be written as

$$F(z) = \phi(x, y) + i\psi(x, y) \quad \text{…. 11.13}$$

Consequently, *F(z)* conformally maps the curves in the *z*-plane onto the corresponding curves in the *w*–plane and vice-versa preserving the angles during mapping.

Since, both the real and imaginary parts of *F(z),* viz. $\phi(x, y)$ and $\psi(x, y)$, are harmonic functions, they satisfy Laplace's equation and hence either one of these two could be used to find potential. Thus the complex analytic function *F(z)* is known as complex potential. Laplace's equation is one of the most important partial differential equations in engineering and physics. The theory of solutions of Laplace's equation is known as Potential Theory. The concept of complex potential relates potential theory closely to complex analysis.

If $\phi(x, y)$ is considered to be real potential, then $\phi(x, y) = const$ represents equipotential lines in the *z*-plane. Since, $\phi(x, y)$ and $\psi(x, y)$ are orthogonal, hence, $\psi(x, y) = const$ represents electric field lines in the *z*-plane. For example, consider the complex potential function as $F(z) = Az + B = Ax + B + iAy$. Then the equipotential lines corresponding to $\phi(x, y) = Ax + B = const$ are straight lines parallel to *y*-axis and the electric field lines corresponding to $\psi(x, y) = Ay = const$ are straight lines parallel to *x*-axis.

The introduction of the concept of complex potential is advantageous in the following ways: i) it is possible to handle equipotential and electric field lines simultaneously and ii) Dirichlet problems with difficult geometry of boundaries could be solved by conformal mapping by finding an analytic function *F(z)* which maps a complicated domain Ω in the *z*-plane onto a simpler domain Ω' in the *w*-plane. The complex potential $F'(w)$ is solved in the *w*-plane by satisfying Laplace's equation along with the boundary conditions. Then the complex potential in the *z*-plane can be obtained by inverse transform from which the real potential is obtained as $\phi(x, y) = \mathrm{Re}\{F(z)\}$. This is a practicable way of solution as harmonic functions remain harmonic under conformal mapping.

Procedural Steps in Solving Problems using Conformal Mapping

1) Find an analytic function *w=F(z)* to map the original region Ω in the *z*-plane to the transformed region Ω' in the *w*-plane. The region Ω' should be a region for which explicit solutions to the problem at hand are known.
2) Transfer the boundary conditions from the boundaries of the region Ω in the *z*-plane to the boundaries of the transformed region Ω' in the *w*-plane.
3) Solve the problem and find the complex potential $F'(w)$ for the transformed region Ω' in the *w*-plane.
4) Map the solution $F'(w)$ for the region Ω' in the *w*-plane back to the complex potential *F(z)* for the region Ω in the *z*-plane through inverse mapping.

The steps are schematically shown in Fig.11.5. The most important step is to find an appropriate mapping function *w=F(z),* which fits the problem at hand. Once the right mapping function has been found, the problem is as good as solved.

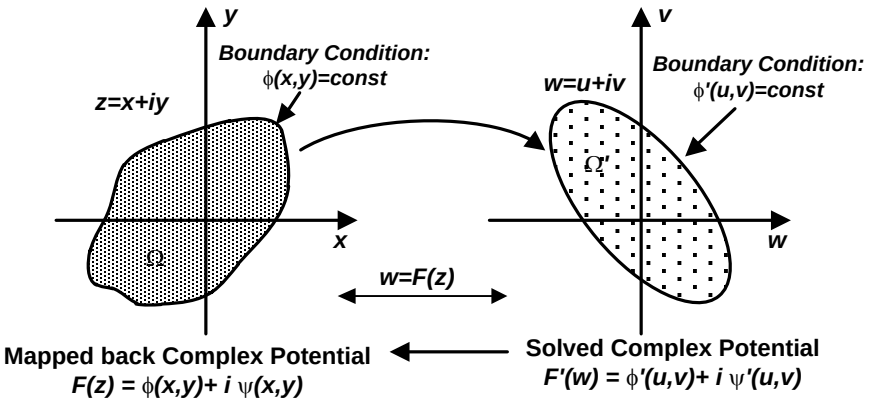

Fig.11.5 Schematic representation of solution of potential problem by conformal mapping

Applications of Conformal Mapping in Electrostatic Potential Problems

Conformal mapping is a powerful method for solving boundary value problems in two-dimensional potential theory through transformation of a complicated region into a simpler region. Electric potential satisfies Laplace's equation in charge free region. Therefore, electrostatic field that satisfies Laplace's equation in a two-dimensional region in *xy*-plane, will also satisfy Laplace's equation in any plane to which the region may be transformed by an analytic complex potential function *F(z)*. For each value of complex $z = x + iy$, there is a corresponding value of complex $w = F(z)$. In other words, for every point in the *z*-plane, there is a corresponding point in the *w*-plane. As a result, the locus of any point in the *z*-plane will trace another path in *w*-plane. Let, the locus in the *z*-plane maps onto a path $\phi'(u,v) = const$ in the *w*-plane, which corresponds to an equipotential and may also be the surface of a conductor. Then the problem can be solved in the *w*-plane incorporating the appropriate boundary condition, i.e. the value of the conductor potential, and the results can be mapped back to *z*-plane to get the real potential and then the electric field lines can be obtained from the conjugate harmonic function. This section discusses some of the applications of conformal mapping in solving two-dimensional electrostatic potential problems.

Conformal Mapping of Co-Axial Cylinders

The cross-sectional view of a single-core cable is shown in Fig.11.6, where the co-axial cylindrical conductors are of infinite length in the direction normal to the plane of the paper. Hence, the field varies only in the cross-sectional plane and is translationally invariant in the direction of the length of the cable. Let, the cross-sectional plane of the cable be the *x*-*y* plane or the *z*-plane. Then the field in the region between the two cylindrical conductors can be found by conformal mapping. Let, the radii of the inner and the outer conductors be r_1 and r_2, respectively, and the potential of the inner and the outer conductors be *V* and zero respectively.

Consider the complex analytical function for conformal mapping be

$$w = u + iv = C_1 \ln(z) + C_2 \quad \text{…. 11.14}$$

where, $z = x + iy = re^{i\theta}$ such that $r = \sqrt{x^2 + y^2}$ and $\theta = \tan^{-1}(y/x)$

So, $u + iv = C_1 \ln(re^{i\theta}) + C_2 = C_1 \ln r + C_2 + iC_1\theta$

or, $u = C_1 \ln(r) + C_2$ and $v = C_1\theta$ …. 11.15

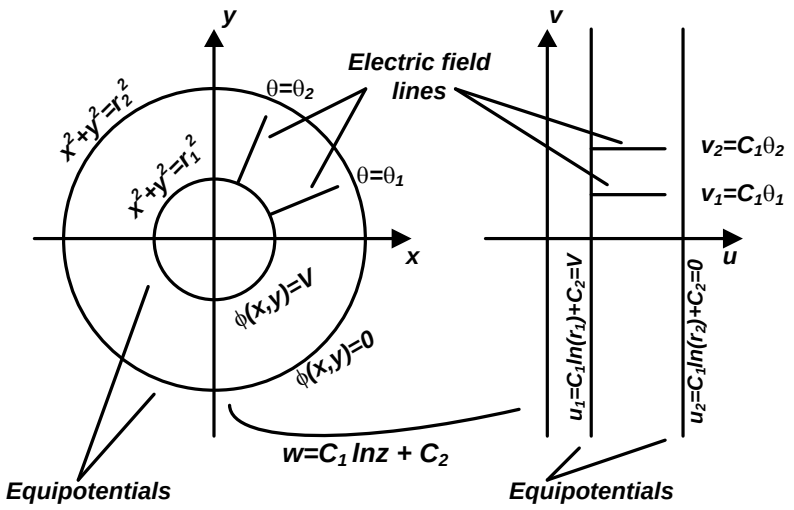

Fig.11.6 Conformal mapping of co-axial cylinders

For the inner conductor, $x^2+y^2=r_1^2$ and hence it maps to a straight line $u_1 = const$ parallel to *v*-axis in the *w*-plane. Similarly, the outer conductor for which $x^2+y^2=r_2^2$ maps to another straight line $u_2 = const$ parallel to *v*-axis in the *w*-plane, as shown in Fig.11.6. In other words, the field within the two cylindrical conductors in the *z*-plane is conformally mapped to field between two infinitely long parallel plates, i.e. the field within a parallel-plate capacitor, in the *w*-plane. From Fig.11.6 it may be seen that the orthogonality of the equipotentials in the form of circles and electric field lines in the form of radial lines in the *z*-plane are maintained in the *w*-plane, where the equipotentials are straight lines parallel to *v*-axis and the electric field lines are straight lines parallel to *u*-axis.

From the boundary conditions on the conductor surfaces

$$C_1 \ln r_1 + C_2 = V \qquad \text{…. 11.16}$$

and $C_1 \ln r_2 + C_2 = 0$ …. 11.17

From eqns. (11.16) and (11.17),

$$C_1 = -\frac{V}{\ln \frac{r_2}{r_1}} \quad \text{and} \quad C_2 = \frac{V \ln r_2}{\ln \frac{r_2}{r_1}} \qquad \text{…. 11.18}$$

The potential at any radius *r* is given by $u = C_1 \ln r + C_2$. Correspondingly, in the *z*-plane

$$\phi(x,y) = -\frac{V \ln r}{\ln \frac{r_2}{r_1}} + \frac{V \ln r_2}{\ln \frac{r_2}{r_1}} = \frac{V \ln \frac{r_2}{r}}{\ln \frac{r_2}{r_1}} \qquad \text{…. 11.19}$$

Then, $E_r(x,y) = -\frac{\partial \phi}{\partial r} = \frac{V}{r \ln \frac{r_2}{r_1}}$ …. 11.20

Eqn.(11.20) gives the value of electric field intensity at any radius *r*, which is the same as the one given by eqn.(4.30).

Graphical Field Plotting

Introduction

Most of the practical problems have such complicated geometry that no exact method of finding the electric field is possible or feasible and approximate techniques are the only ones which can be used. Out of the several approximate techniques, numerical techniques are now extensively used to determine electric field distribution with high accuracy. Numerical techniques, which are widely used, will be discussed in details in the later chapters. In this chapter, experimental and graphical field mapping methods are discussed. Experimental field mapping involve special equipments such as electrolytic tank, a device for fluid flow, conducting paper and associated measuring system. The other mapping method is a graphical one and needs only paper and pencil. In both these methods, the exact value of the field quantities could not be determined, but accuracy level which is sufficient for practical engineering applications could be achieved. Graphical field plotting is economical compared to experimental method and is also capable of providing good accuracy when used with skill. Accuracy of the order of 5 to 10% in capacitance determination could be achieved even by a non-expert simply by following the rules.

Experimental Field Mapping

Experimental method of field mapping is based on the analogy of stationary current field with static electric field, as presented in Table 12.1, rather than directly on measurement of electric field. If the medium between electrodes is isotropic, then volume conductivity and dielectric constant do not vary with position. Then current density (J) in stationary current field and electric field intensity (E) and electric flux density (D) in static electric field will be in the same direction. In other words, current density and electric field lines are the same. Thus for a given electrode system, if a slightly conducting material, e.g. conducting paper or an electrolyte, is placed instead of a dielectric material between the electrodes, then electric field lines and equipotential lines will remain the same.

It is well known that if one travels along a line through an electric field and measures electric scalar potential V as one goes, then the negative of the rate of change of V is equal to the component of electric field intensity E in the direction of travel. In other words,

$$\vec{E} = -\frac{\partial V}{\partial l}\hat{u}_l \qquad \text{…. 12.1}$$

If $-\frac{\partial V}{\partial l}$ is maximum, then it gives the value of E itself. If electric potential does not change with position, then the path of travel is at right angles to the electric field and is along an equipotential. Thus electric field could be mapped by a voltmeter that will measure potential difference and two metal rods acting as probes. The probes are connected to the terminals of the voltmeter and are placed in various positions in an electric field to monitor the potential differences between the positions of the two probes.

Table 12.1 Analogy between static electric field and stationary current field

Static Electric Field	Stationary Current Field
Electric Flux	Electric Current
$\vec{D}=\varepsilon\vec{E}$	$\vec{J}=\kappa\vec{E}$
Dielectric constant	Volume conductivity
$Q=\oint_S \vec{D}.d\vec{s}$	$I=\oint_S \vec{J}.d\vec{s}$

For the determination of equipotential lines one probe is kept still, while the other probe is moved. In whichever position of the moving probe the voltmeter registers a zero reading; the potential of the moving probe is same as that of the standstill probe. By marking each such position, equipotentials could be traced.

For tracing electric field lines the two probes are kept at a constant separation distance and one probe is rotated around the other. The position of the rotating probe where the voltmeter registers a maximum reading, the electric field is changing at its maximum rate. Hence, the electric field at that location of the rotating probe is parallel to the line joining the two probes. By repeating this measurement process at several positions, the electric field could be mapped.

Since a real-life voltmeter draws a current, however small it may be, measurement of the potential differences using voltmeter could not be done with vacuum or air as the medium. In practice, measurement is carried out for the electric field that is set up in a medium, which is slightly conducting.

Commonly slightly conducting paper, e.g. paper impregnated with carbon, is used. Since the paper is slightly conducting, the electric field due to the charged electrodes is almost the same as the one that would be produced in air or vacuum with similar geometry. At the same time the paper is sufficiently conducting to supply the small current needed by the voltmeter.

Alternately electrolytic tank setup is used which consists of a specially fabricated insulating tray. A large sheet of laminated graph paper is pasted on the base plate of the tray. The tray is then half-filled with an electrolyte and the height of the electrolyte is kept same throughout the tray. Metallic electrodes are placed in the electrolytic tank, which are shaped to conform to the boundaries of the problem, and appropriate potential difference between the electrodes is maintained.

Field Mapping using Curvilinear Squares

Field mapping by curvilinear squares is a graphical method based on the orthogonal property of a pair of conjugate harmonic functions and also on the geometric considerations. This method is suitable for mapping only those fields in which there is no variation of field in the direction normal to the plane of the sketch, i.e. the field is two-dimensional in nature. Many practical electric field problems may be considered as two dimensional, e.g. the co-axial cylindrical system or a pair of long parallel wires. In these cases the field remains same in all cross-sectional planes. It is a fact that no real system is infinitely long, but the idealization is a useful one for electric field analysis and visualization.

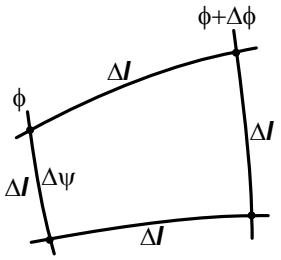

Fig.12.1 A typical curvilinear square

In this method the field region of interest is discretized into a network of curvilinear squares formed by flux or field lines and equipotentials. Curvilinear square is a planar geometric figure which is different from a true square as its sides are slightly curved and slightly unequal, but which approaches a true square as its dimensions become small. A typical curvilinear square is shown in Fig. 12.1. The field map thus obtained is unique for a given problem and helps in understanding the behaviour of electric field through visualization. The method of curvilinear square is capable of handling problems with complicated boundaries. A curvilinear field map is also independent of field property coefficients and could be directly applied from one physical field to another if an analogy exists between the concerned fields.
Theoretically curvilinear field mapping is based on Cauchy-Riemann relations, which ensures that the Laplace's equation is satisfied by a conjugate pair of harmonic functions in any orthogonal coordinate system. Hence, this method utilizes the fieldline coordinate representation of electric field such that electric field is always tangent to the fieldlines and depends only on the distribution of fieldlines and equipotentials.

Foundations of Field Mapping

Construction of field map using curvilinear squares is based on some significant features of electric field as described below:
i) A conductor boundary is one of the equipotentials.
ii) Equipotential and electric field intensity (or electric flux density) are normal to each other. As a conductor boundary is an equipotential, hence electric field intensity and electric flux density vectors are always perpendicular to the conductor boundaries.
iii) Electric flux lines (often termed as streamlines) originate and terminate on charges. Hence, in the case of a homogeneous and charge free dielectric medium, electric flux lines originate and terminate on conductor boundaries.
Fig.12.2 shows two coaxial cylindrical conductor boundaries having a specified potential difference (V) and extending 1m into the plane of the paper. A field line is considered to leave the boundary with more positive electric potential making an angle of 90^0 with the boundary at the point X. If the line is extended following the rule that it is always perpendicular to the equipotentials and if the dielectric medium is considered to be homogeneous and charge free, then the fieldline will terminate normally on the boundary of the less positive conductor at the point X' as shown in Fig.12.2. In a similar manner, another fieldline could be drawn in such a way that it starts from the point Y on the more positive conductor boundary and terminates on the point Y' on the less positive conductor boundary. As the fieldlines are drawn perpendicular to the equipotentials everywhere, electric field intensity and hence electric flux density will be tangent to a fieldline everywhere on it. Consequently, no electric flux can cross any fieldline thus drawn. Therefore, if there is a charge of ΔQ on the surface of the conductor between the points X and Y, then a flux of $\Delta\psi = \Delta Q$ will originate in this region and must terminate on the surface of the other conductor boundary between the points X' and Y'. Such a pair of fieldlines is known as a

"*flux tube*" as it seems to carry flux from one conductor to the other without losing any flux in between the two conductors. For simplification of interpretation of the field map, another flux tube *YZ* may be drawn in such a way that the same amount of flux is carried in the flux tubes *XY* and *YZ*. The method of determination of dimensions of the curvilinear square for drawing such flux tubes is described in the next section.

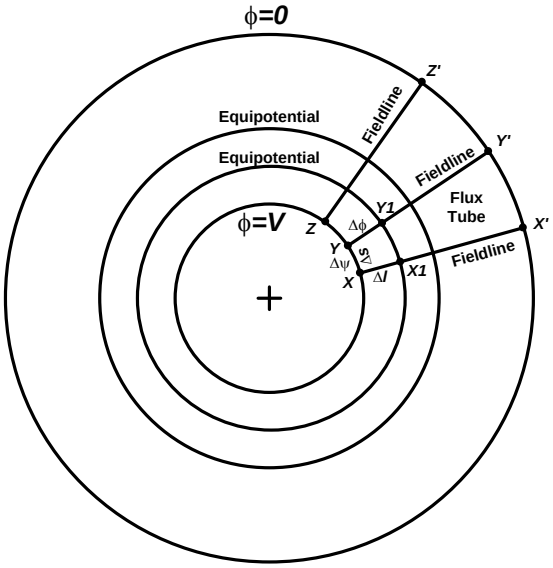

Fig.12.2 Field map between two co-axial cylinders

Sketching of Curvilinear Squares

Considering the length of the line joining the points *X* and *Y* to be Δs, the flux in the tube *XY* to be $\Delta\psi$ and the depth of the tube to be 1m into the paper, the electric flux density at the midpoint of this line is then given by

$$D = \frac{\Delta\psi}{\Delta s} \qquad \text{…. 12.2}$$

So, considering the permittivity of dielectric medium to be ε, electric field intensity at the midpoint of the line *XY* is then given by

$$E = \frac{1}{\varepsilon}\frac{\Delta\psi}{\Delta s} \qquad \text{…. 12.3}$$

Alternately, electric field intensity could also be determined from the potential difference between the points *X* and *X1* lying on the same fieldline on two equipotentials as shown in Fig.12.2.

Considering the length of the line joining the points *X* and *X1* to be Δl and the potential difference between the two consecutive equipotentials to be $\Delta\phi$, electric field intensity at the midpoint of the line *X-X1* is then given by

$$E = \frac{\Delta\phi}{\Delta l} \qquad \text{…. 12.4}$$

Considering Δs and Δl to be small, the two values of electric field intensity as given by eqns. (12.3) and (12.4) may be taken to be equal. Hence,

$$\frac{1}{\varepsilon}\frac{\Delta\psi}{\Delta s} = \frac{\Delta\phi}{\Delta l}$$

or, $$\frac{\Delta l}{\Delta s} = \varepsilon\frac{\Delta\phi}{\Delta\psi} \qquad \text{…. 12.5}$$

For sketching the field map, consider the following: a) homogeneous dielectric having a constant permittivity ε, ii) constant amount of electric flux per tube, i.e. $\Delta\psi$ is constant, and iii) constant potential difference between two consecutive equipotentials, i.e. $\Delta\phi$ is constant. Then from eqn.(12.5), $\frac{\Delta l}{\Delta s} = constant$. In other words, the ratio of the distance between fieldlines as measured along an equipotential and the distance between equipotentials as measured along a fieldline must be maintained constant and not the individual lengths. The simplest ratio of lengths that can be maintained is unity, so that $\Delta l = \Delta s$. Then the field region is divided into curvilinear squares by the fieldines and equipotentials.

The field map thus obtained is composed of curvilinear squares of the same kind such that each square has the same potential difference across it and also has the same amount of flux through it. For a given $\Delta\phi$ and $\Delta\psi$, the sides of a curvilinear square are thus inversely proportional to electric field intensity. For a non-uniform field electric field intensity varies with location and hence Δl and Δs vary with the strength of electric field. In the region of higher field strength, Δl and Δs are to be kept small, i.e. the squares are to be made smaller in size where the magnitude of the field intensity is high. On the other hand, the squares are made larger in size in the field region where the field intensity is low.

It may be recalled that the product of electric charge and electric potential difference is the energy of electric field. Moreover, electric charge and electric flux has a one to one correspondence. Thus for a field map if $\Delta\phi$ and $\Delta\psi$ are kept constant, then their product remains constant and hence, energy of electric field remains constant. Therefore, curvilinear squares having the same ratio as give by eqn.(12.5) have the same energy stored in electric field regardless of the size of the square. A curvilinear square can thus be scaled up or down keeping the energy stored in the curvilinear square unaltered as long as the ratio given by eqn.(12.5) remains unaltered.

Construction of Curvilinear Square Field Map

The fieldines and equipotentials are typically drawn on the original sketch which shows the conductor boundaries. Arbitrarily one fieldline is begun from a point on the surface of the more positive conductor with a suitable value of Δl and an equipotential is drawn perpendicular to the fieldline with a value of $\Delta s = \Delta l$. Then another fieldline is added to complete the curvilinear square. The field map is then gradually extended throughout the field region of interest. As the field map is extended, the condition of orthogonality of fieldline and equipotential should be kept paramount, even if this results in some squares with ratios other than unity. Construction of a satisfactory field map using curvilinear squares is a trial and error process that involves continuous adjustment and refinement. Typically the field maps are started as a course map having large curvilinear squares. Then the field map is fine tuned through successive subdivisions to form a dense field map having higher accuracy. In the process of subdivision, the lengths between consecutive fieldlines as well as equipotentials are kept equal. Before starting the construction of a field map, it is a judicious practice to examine the geometry of the system and take advantage of any symmetry that may exist in the system under consideration. This is because of the fact the lines of symmetry serve as boundaries with no flux crossing and thereby separate regions of similar field maps.

Capacitance Calculation from Field Map

Once the field map is drawn, it is possible to determine the capacitance per unit length between the two conductors using the field map. It is well known that capacitance between

two conductors having a potential difference of V is given by $C = \frac{Q}{V}$, where Q is the charge on the conductor. Applying Gauss's law on a Gaussian surface enclosing the conductor having more positive potential, $Q = \psi$, where ψ is the flux coming out of the conductor. Thus, $C = \frac{\psi}{V}$.

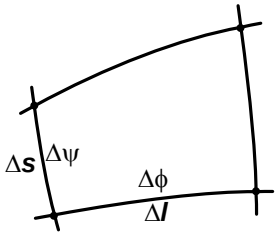

Fig.12.3 An isolated curvilinear rectangle

To calculate the capacitance with the help of curvilinear rectangle, consider first an isolated curvilinear rectangle as shown in Fig.12.3. Let the flux through it be $\Delta\psi$ and the potential difference across it be $\Delta\phi$. Considering the curvilinear rectangle to be small, the flux density may be assumed uniform within the curvilinear rectangle so that

$$\Delta\psi = \varepsilon E \Delta s \times 1 \quad \text{…. 12.6}$$

where, the depth is taken to be 1m into the plane of the field map.

Electric field intensity (E) and the potential difference $\Delta\phi$ are related as

$$\Delta\phi = E \times \Delta l \quad \text{…. 12.7}$$

Combining eqns. (12.6) and (12.7)

$$\Delta\psi = \varepsilon \Delta s \times \frac{\Delta\phi}{\Delta l}$$

Therefore, the capacitance of the small curvilinear rectangle, which may be taken as a small field cell, is given by

$$\Delta C = \frac{\Delta\psi}{\Delta\phi} = \varepsilon \frac{\Delta s}{\Delta l} \quad \text{…. 12.8}$$

The total amount of flux (ψ) emanating from one conductor and terminating on the other conductor may be obtained by adding all the small amounts of flux ($\Delta\psi$) through each flux tube so that

$$\psi = \sum_{N_\psi} \Delta\psi = N_\psi \Delta\psi \quad \text{…. 12.9}$$

where, $\Delta\psi$ is assumed to be same for each flux tube and N_ψ is the number of flux tubes in parallel, i.e. the number of curvilinear rectangles in parallel.

The total potential difference between the two conductors (V) may be obtained by adding all the small amounts of potential differences ($\Delta\phi$) between consecutive equipotentials starting from one conductor and finishing at the other conductor, i.e.

$$V = \sum_{N_\phi} \Delta\phi = N_\phi \Delta\phi \quad \text{…. 12.10}$$

where, $\Delta\phi$ is assumed to be same between any two consecutive equipotentials and N_ϕ is the number of equipotentials (including the two conductors) minus one, i.e. the number of curvilinear rectangles in series between the two conductors.

Thus capacitance per unit length of the two conductors is given by

$$C = \frac{\psi}{V} = \frac{N_\psi}{N_\phi}\frac{\Delta\psi}{\Delta\phi} = \frac{N_\psi}{N_\phi}\frac{\varepsilon\Delta s}{\Delta l} = \varepsilon\frac{N_\psi}{N_\phi} \quad \text{…. 12.11}$$

where, $\Delta s = \Delta l$, considering the ratio of the lengths to be unity, i.e. considering curvilinear squares.

Hence, determination of capacitance from the field map involves counting of curvilinear squares in two directions, one in series between the two conductors and the other in parallel around either conductor.